# Age and Geochemistry of the Mafic Sills, ODP Site 1276, Newfoundland Margin

**S. R. Hart and J. Blusztajn**

**Woods Hole Oceanographic Institution, Woods Hole, 02543**

Keywords: Site 1276, rift magmatism, continental rifting, Newfoundland margin, Leg 210.

## Abstract

Site 1276, Leg 210 of the Ocean Drilling Program, was located on the Newfoundland margin in seismically-defined ~128 Ma "transitional" crust just west of presumed oceanic crust, and the M3 magnetic anomaly. The goal of drilling on this non-volcanic margin was to study the rifting, nature of basement, and post-rift sedimentation in the Newfoundland-Iberia rift. Drilling of this 1739m hole was terminated 90-160 meters above basement, in the lower of a doublet of alkaline diabase sills. We have carried out geochemical studies of the sill complex, in the hopes that they will provide proxy information regarding the nature of the underlying basement. Excellent $^{40}Ar/^{39}Ar$ plateau ages were obtained for the two sills: upper sill ~ 105.3 Ma; lower sill ~ 97.8 Ma. Thus the sills are substantially younger than the presumed age of the seafloor at site 1276 (~ 128 Ma), and were intruded beneath substantial sediment overburden (250 m for the upper, older sill, and 575 m for the lower younger sill). While some of the geochemistry of the sills has been compromised by alteration, the "immobile" trace elements show these sills to be hawaiites, differentiated from an enriched alkaline or basanitic parentage. Sr, Nd and Pb isotopes are suggestive of an enriched hotspot/plume mantle source, with a possible "added" component of continental material. These sills unequivocally were not derived from typical MORB (asthenospheric) upper mantle.

## Introduction

The processes by which new oceanic crust is formed during continental rifting have been debated for decades. Rifted margins are classified as volcanic or non-volcanic (White et al., 1987; Mutter, 1993), but the source and nature of the magmatism that can accompany either type of margin remains enigmatic. Are the first magmatic products simply derived from the sub-continental lithospheric mantle that abuts the rifting (Hawkesworth et al., 1999, 2000), or is melting only possible once active upwelling of asthenospheric (MORB) mantle becomes energetic (Mutter et al., 1988; Keen et al., 1994; Rohrman and van der Beek, 1996)? Is such small-scale upwelling even dynamically possible (King and Anderson, 1998)? Does rift-related magmatism require local mantle thermal anomalies, thus implicating mantle plumes as sources for early rift magmatism (White and McKenzie, 1989; Leitch et al., 1998)? These three mantle sources (sub-continental lithosphere, depleted MORB asthenosphere, mantle plumes) have different trace element and isotopic fingerprints, so in principle are distinguishable.

The abyssal Newfoundland basin spans the transition from known continental crust to known oceanic crust (Hopper et al., 2004). Ocean Drilling Program Leg 210, Site 1276, was drilled in ~128 my transitional crust on this non-volcanic margin, to constrain the rifting, nature of basement, and post-rift sedimentation in the Newfoundland-Iberia rift; Figure 1 (Tucholke, B.E., Sibuet, J.-C., Klaus, A., et al., 2004; Shipboard Scientific Party, 2004). A downhole lithology log may be found in the latter reference. While drilling terminated 90-160 meters above true basement, several diabasic sills were cut near the bottom of the 1739 m hole, and these may provide a proxy for basement magmatism in this rift (identification of these bodies as sills rests on the recovery of a baked upper contact for the upper body, and the ages reported below that show both bodies are substantially younger than the enclosing sediment). We show that these sills post-date the rifting and formation of basement by some 25 my years, and are definitely not of MORB pedigree, but are rather of "plume-like" geochemistry.

## Methods

Ten core samples from the upper sill and 7 from the lower sill were thin-sectioned and studied petrographically; sample numbers, depths and a brief petrography are given in Table 1. From these samples, three core sections were selected from each sill (weighing from 47 to 120 grams; these six samples are hereafter referred to only by their core and section number, bold

font in Table 1) and fragmented into sub-cm size chips. The degree of alteration is moderate in these samples, ranging from perhaps 25-40%. The freshest available material was hand-picked under a binocular microscope; several grams were sent to Bob Duncan's lab at Oregon State University for $^{40}Ar/^{39}Ar$ analysis, and the remainder was powdered in an agate mill. A split of this powder was analyzed for major and trace elements (XRF and ICP) at the GeoAnalytical Lab, Washington State University. A sub-sample of this powder was leached for 1 hour in hot 6N HCl, repeatedly rinsed in pure water, and used for Sr, Nd and Pb isotopic analysis (Taras and Hart, 1987). In addition, a split of this leached powder was also analyzed for trace elements at the GeoAnalytical Lab, WSU.

The precision (1σ) for major elements in basalts by XRF is 0.11 - 0.33% of the amount present ($SiO_2$, $Al_2O_3$, $TiO_2$, $P_2O_5$) and 0.38 - 0.71% (other elements). For Ba, Rb, Sr, Zr and Y by XRF, the precision is 0.5 – 3.1% (1σ); see Johnson et al. (1999) for the XRF techniques, the precision of other trace elements, and for evaluation of accuracy for majors and traces based on analyses of international standards. For trace element analyses by ICP-MS, the precision for basalts is 0.77 – 3.2% (1σ) for all elements except Th (9.5%) and U (9.3%); see Knaack et al. (1994) for the ICP-MS techniques, and evaluation of accuracy based on analyses of international standards.

Sr and Nd chemistry was done with conventional ion chromatography, using DOWEX 50 cation resin, and HDEHP-treated teflon for Nd separation (Taras and Hart, 1987). Pb chemistry utilized the HBr-$HNO_3$ procedure of Galer (1986) and Abouchami et al. (1999), with a single column pass. Sr, Nd and Pb analyses were done on the NEPTUNE multi-collector ICP-MS at WHOI. For Sr and Nd, the internal precision is 5-10 ppm (2σ); external precision, after adjusting to 0.710240 and 0.511847 for the SRM987 and La Jolla Nd standards respectively, is estimated to be 15-25 ppm (2σ). Further details may be found in Jackson and Hart (2006) and Hart et al (2005). Pb analyses carry internal precisions on XXX/204 ratios of 15-30 ppm; SRM997 Tl was used as an internal standard, and external reproducibility (including full chemistry) ranges from 17 ppm (2σ) for $^{207}Pb/^{206}Pb$, to 117 ppm (2σ) for $^{208}Pb/^{204}Pb$ (Hart et al., 2002; 2004). Pb ratios were adjusted to the SRM981 values of Todt et al. (1996); two separate lots of the SRM981 standard were inter-compared and any possible isotopic heterogeneity between these lots was <10 ppm for XXX/204 ratios, and <1.5 ppm for $^{208}Pb/^{206}Pb$ ratios.

**Classification and Alteration**

Major element, trace element and isotope data are given in Table 2. If the major element chemistry is taken at face value, both sills are clearly alkalic, and would be classified as alkali basalt-hawaiite on a conventional alkali-silica plot; see Fig. 2. Only sample 88-5 plots below the "main cluster"; this sample has high Ba and volatiles and is more altered than the others (see below). The high $TiO_2$ (3.5%-3.6%) also supports a classification as a differentiated basanite. Mg-Numbers range from 0.42-0.44 for the lower sill, and 0.52-0.53 for the upper sill, consistent with significant differentiation, and location in the hawaiite field.

Primary Cpx phenocrysts from samples 88-5 and 99-6 were analyzed by electron probe to further constrain the composition of the sills prior to any alteration (Supplementary Data, Table 1). The $Al_2O_3$and $TiO_2$ contents show systematic co-variations, Fig. 3, with the clinopyroxenes from the upper sill sample containing a slightly lower $CaTiAl_2O_6$ component. More importantly, this plot serves as a robust discriminator between alkali basalts and N-MORBS, as the $TiO_2$ contents of clinopyroxenes from N-MORBS are distinctly lower than the clinopyroxenes from the sill samples, Fig. 3. This is a simple reflection of the lower $TiO_2$ contents of N-MORB melts (~1.5%) compared to the sill whole rocks (3.5%-3.6%).

However, there is also clear evidence of open-system behavior for some elements during the extensive alteration that these mafic sills have undergone. For example, the Ba contents in the upper sill can be very high (up to 4900 ppm!), and this Ba is located in the abundant acicular secondary apatite that is especially prevalent in the upper sill (Table 1). This high Ba is correlated with low $Na_2O$, and the low $Na_2O$ is itself correlated with high volatile contents (up to 3%); see Fig. 4. We suggest that the primary $Na_2O$ contents were all similar (~ 3.8%), and that loss of Na has occurred during plagioclase alteration. "Restoring" this Na would shift the upper sill data on Fig. 2 upward by 0.5-1%, making these samples even more alkalic. There is no obvious correlation of $K_2O$ with Ba, Na or volatiles, suggesting that $K_2O$ has been less affected by alteration. This obviously is important in understanding the $^{40}Ar/^{39}Ar$ geochronology.

Splits of the powdered samples were strongly leached, in an attempt to remove alteration phases prior to isotope analysis. This is a common procedure in the isotopic analysis of old and altered basalts (Cheng et al., 1987; Mahoney et al., 1987; Taras and Hart, 1987). A comparison of the leached and unleached trace element concentrations may provide clues as to the nature of the alteration phases, and their impact on the geochemistry of these sills. Fig. 5 is a plot of the

ratio of the leached concentration of the trace elements to the concentrations in the whole rock (unleached) powder. Elements plotting on or above the 1.0 line are those unaffected by leaching, or "concentrated" in the residual powder. These include the elements normally classified as "immobile" (Th, Nb, Ta, Zr, Hf). It is interesting that Rb and U, elements that are usually susceptible to alteration, are also relatively immobile. However, the Ba that was added to the upper sill during alteration is not significantly "removable" by leaching (whereas the Cs is). In other words, lack of "leachability" does not infer lack of alteration. Pb, Sr and Eu in the upper sill samples are less affected by leaching than in the lower sill samples, perhaps reflecting their hosting in plagioclase. While the abundance of groundmass plagioclase is comparable in both sills, the upper sill does have small quantities of distinctly larger plagioclase phenocrysts that may be more resistant to the leaching procedure.

Also note that the REE, normally considered immobile elements, are strongly leached in all cases, and comparable to Cs and K in this regard. The inference then is that the REE, Cs and K are contained in phases that are leachable, but that are not hosts for the "unleached" elements such as Rb, Ba, Th, U, Nb, Ta, Zr and Hf. While a glassy or fine-grained mesostasis might be considered as a candidate for a leachable REE-containing phase, this should also provide leachable Rb, Ba, Th, etc., whereas these elements do not appear to be leachable. It might be inferred that a large fraction of the REE have been added during alteration, and are contained in leachable REE-specific phases such as rhabdophane. This REE-phosphate is common as an alteration product in subaerial basalts (Fodor et al., 1989; Cotten et al., 1995), and is acid-soluble. The presence of secondary apatite in the upper sill is evidence that phosphorous was available in the alteration fluids. To our knowledge, however, rhabdophane has not been reported as an alteration product in submarine settings. Also, the whole-rock spidergrams, to be discussed below, give no indication that the REE are anything but primary magmatic in nature.

**Geochronology**

Ages on two samples from each sill were determined by step-release $^{40}Ar/^{39}Ar$ dating. Despite the moderate alteration state of these samples, the Ar plateaus are excellent, Fig. 6 (data given in Table 2 supplementary material), and the ages meet the four statistically testable criteria given by Duncan and Keller (2004) that are necessary for an age to define an accurate estimate of the time of sample crystallization. The low-temperature Ar fractions (15-20%) are younger

than the high-temperature plateau ages, perhaps indicating time-integrated (open system) Ar loss from a potassic mineral or glass that formed contemporaneously with sill emplacement, or a younger addition of potassic clay minerals from which the Ar was released during the lower temperature steps of the lab heating. Note that 60-80% of the K in the sill samples was leachable, as shown in Fig. 5, suggesting that at least some of the radiogenic Ar might also be loosely-bound.

The two ages for the upper sill agree within ~1% (104.7 ± 1.7 Ma, 105.9 ± 1.8 Ma, 2σ errors), averaging 105.3 Ma. The two ages for the lower sill are younger, and are spread by 3.8 Ma, just at 2σ analytical precision (99.7 ± 1.8 Ma, 95.9 ± 2.0 Ma), averaging 97.8 Ma; the ~ 7.5 Ma difference in measured age between the two sills is highly significant on a statistical basis. The harder question to answer is whether this difference in measured ages also represents a difference in crystallization ages. It could be argued, for example, that the younger age for the lower sill is an "alteration age", caused by a late addition of K. There is little support for this in the trace element geochemistry, however. For example, both the content of K, and the ratio of K to immobile elements such as Nb and Ta is lower in the lower (younger) sill by 35-45% (table 2), as is the K/La ratio (whereas the absolute Nb, Ta and La contents are very similar in the two sills). This is the opposite of what would be expected if the younger lower sill ages are due to late addition of K. Also, various trace element ratios in the lower sill are closer to "canonical" OIB values than those in the upper sill. This is particularly true for the youngest sample (99-6), that has K/La, Rb/Cs, Ba/Rb, K/Rb and Nb/U of 407 (306), 84 (95), 21.5 (11.3), 406 (480) and 51 (52); canonical values are given in parentheses and are from Hofmann and White (1983), Morris and Hart (1983) and Hofmann (2003). While these geochemical considerations may not constitute compelling evidence that the measured $^{40}Ar/^{39}Ar$ ages are in fact crystallization ages, there is little in the geochemistry that argues otherwise. This, along with the excellent $^{40}Ar/^{39}Ar$ plateaus, leads us to accept the measured ages as crystallization ages.

It follows then that the sills are not related to the same magmatic event. This is substantiated by the isotopic and trace element data (see below) that also show that these two sills, while familial, are not strictly co-genetic.

The sills are substantially younger than the presumed age of the seafloor at Site 1276 (just west of M3 anomaly, ~ 128 Ma; Tucholke, Sibuet, Klaus et al., 2004), and they are also younger than the host sediments (~ 111 Ma at upper sill depth, > 115 Ma (?) at lower sill depth). There

was ~ 250m of sedimentary overburden when the upper (older) sill was intruded, and ~ 575m when the lower sill was intruded (using the nannofossil-based age-depth curve, Figure 141 in: Shipboard Scientific Party, 2004).

**Trace element geochemistry**

The easiest way to illustrate the overall chemistry of the two sills is with a trace element abundance plot (or "spidergram"), Fig. 7. On this plot, the two sills appear very similar in geochemistry, with the exception of Cs, Ba, Pb and Sr. Cs is very susceptible to alteration, and we have already commented on the Ba alteration anomaly. The Pb isotopes are very well behaved (i.e. Pb is not significantly affected by alteration; see below), thus we suggest the difference in Pb between the two sills may relate to variable control of Pb by sulfide during melting and/or differentiation (Hart and Gaetani, 2006). The Sr is variable within each sill, as well as between the sills; the high Sr in the lower sill is also very leachable (Fig. 5), suggesting containment in carbonate. However, carbonate is petrographically much more apparent in the upper sill.

Also shown on the spidergram plot, for comparison, is a pattern for oceanic EM2 basalts, as representative of enriched oceanic "hotspot" volcanism. From La to Lu, the EM2 pattern is very similar to the patterns of the sills. For the more incompatible elements, the sills lack the negative K anomaly (ubiquitous in all oceanic basalts, including MORB), and the peak at Nb-Ta. Except for the Cs and Ba alteration anomalies, the sills also appear generally more depleted than EM2 basalts in U and Th. While the lower Nb and Ta in the sills is suggestive of basalts that have experienced some contamination by continental materials, the low U and Th (and Rb) are inconsistent with crustal components. It is more likely that the sills simply reflect a somewhat higher degree of partial melting of a fairly "garden variety" OIB-type source. What is unambiguously clear is that these basalts are not related to MORB.

To further quantify this geochemical comparison, Fig. 8 compares several specific trace element indicators in the sills with a sampling of "end-member" oceanic basalts, and various continental materials. La/Sm is an index of the degree of incompatible-element enrichment (mantle source composition, plus modification during melting), showing that the sills are much more "enriched" than N-MORB, but less enriched than oceanic hotspot (plume) basalts from EM1, EM2 or HIMU islands. Nb/Nb* measures the abundance of Nb relative to the normalized

average of Th and La (Nb*). The well-known deficiency of high-field-strength elements, such as Nb, in continental materials, is indicated by low Nb/Nb* values. The Site 1276 sills are in fact quite normal in Nb/Nb* compared to oceanic basalts, and in this respect do not have a discernable "continental" signature.

So far we have shown that the Site 1276 sills are clearly not MORB and, while broadly similar to oceanic hotspot basalts, they are also different from these in detail. A more relevant comparison would be with Mesozoic rift-related basalts and diabases from the coastal region of northeastern North America (Jansa and Pe-Piper, 1988, McHone, 1992, Pe-Piper et al., 1990,1992, 1994). Unfortunately, most studies of these rocks do not contain comprehensive high-quality trace element data, or the state of preservation of the rocks is poor. Elements such as Sr, Ba and Zr are the most commonly reported, and are typically fair to good in resistance to alteration. Fig. 9 shows a sampling of this data, in comparison to the Site 1276 sills, from: N-MORB, Mesozoic Appalachian Tholeiites (MAT), and other mafic rift-related volcanics from the Grand Banks, Scotia Shelf, NE Seamounts, Newfoundland Seamounts, Georges Bank, Baltimore Canyon, and average lamprophyres from New England and Quebec. The anomalous Ba in the upper sill is quite obvious on this plot. Otherwise, the sills fall along the crude Zr-Sr and Ba-Sr arrays defined by the other data. The sills are clearly more enriched than the Mesozoic tholeiitic diabases (MAT), though not as enriched as some of the lamprophyres from New England, or those drilled on Georges Bank and Baltimore Canyon. The sills, particularly the upper sill, are quite similar in chemistry to basalts dredged from several of the Newfoundland Seamounts (Sullivan and Keen, 1977); these seamounts lie only 190 km SSW of Site 1276, and they are also close in age (97.7 my; Sullivan and Keen, 1977) to the Site 1276 sills. Karner and Shillington (2005) have noted this temporal equivalence; they also propose that the migration of the Azores, Madeira and Canary plumes across this region between 80-120 my ago is responsible for widespread magmatic activity along this rifted margin. It might also be noted that the Site 1276 locality is directly "downstream" from the Milne Seamounts (see Fig. 1), but the relevance of this possible "connection" must await geochemical work on this hot spot chain.

**Isotope geochemistry**

Here we use the Sr, Nd and Pb isotope data on the sills to "fingerprint" the nature of the mantle source supplying the magmas, and compare the isotopic signature with that of a selection

of North Atlantic hotspots (OIBs). Because of the age of the sills, neither the present day isotope ratios nor the initial (age-corrected) ratios can be directly compared with Sr, Pb and Nd isotopes from the hotspots (most of which are < 5 Ma). Instead we utilize the following scheme (similar to that described in Taras and Hart, 1987): the isotope data for the sills are first corrected back to initial ratios, using the measured $^{40}Ar/^{39}Ar$ plateau ages, and the parent/daughter ratios as measured on the leached powders. It is important to use the leached powder data for this age-correction, because the leached residue that the isotopes were measured on has different parent/daughter ratios than the bulk rock (see Fig. 5). This effect is particularly large for the lower sill samples, due to the very high Th/Pb and U/Pb ratios of these leached powders. These "initial ratios" are then modeled as representing mantle domains that were differentiated at 1.9 Ga from a "bulk earth" mantle (the present day values for our "bulk earth" mantle are fairly conventional: $^{206}Pb/^{204}Pb = 17.879$; $^{207}Pb/^{204}Pb = 15.530$; $^{208}Pb/^{204}Pb = 37.925$; $^{87}Sr/^{86}Sr = 0.70470$; $^{143}Nd/^{144}Nd = 0.512638$). For each sample, a model parent/daughter (mu) ratio was calculated for this evolution from 1.9 Ga to 100 Ma. The initial ratios for each sample were then projected ahead to present using these model parent/daughter ratios. This forward projection is not very sensitive to the assumed age of mantle differentiation.

Table 3 shows a comparison of the Sr, Nd and Pb isotope data as measured on the leached powders, with the calculated initial ratios, and the forward projected model values. For Sr and Nd, the differences between measured and model ratios are minor (50-500 ppm for $^{87}Sr/^{86}Sr$, 27-56 ppm for $^{143}Nd/^{144}Nd$). For the Pb isotopes, the initial ratio correction is large, due to the high U/Pb and Th/Pb ratios of the Core 99 leached powders; this propagates to a significant difference between measured and present model ratios. It is difficult to assess the extent to which these calculated ratios may be affected by alteration effects, either directly in the Pb isotope component, or in the parent/daughter ratios. We note however that the Pb data are remarkably linear in all Pb-Pb plots (measured, initial or model). In addition, the data are well-aligned in U/Pb and Th/Pb isochron plots of the raw measured data (not shown); while the isochron "ages" derived from these arrays do not agree (185 Ma for U/Pb versus 135 Ma for Th/Pb), this simply suggests that the various samples did not have a common Pb isotope composition when the sills formed. This observation is further emphasized by the apparent Pb-Pb isochron age of 395 Ma (for the measured data).

As a further test of possible alteration effects on the isotope data, we analyzed both the leached and unleached powders for $^{87}Sr/^{86}Sr$. We compare these data in terms of initial ratios, as the Rb/Sr ratios in the leached and unleached powders are quite different. This data is reported in Table 3. In 4 of the 6 samples, the initial $^{87}Sr/^{86}Sr$ in the unleached powder is higher, as might be expected for altered basalts in a seawater environment (i. e. sediment pore waters). In one case, the $^{87}Sr/^{86}Sr$ is slightly lower (71 ppm), and in one case it is the same. However, the differences are surprisingly small, the largest being only 540 ppm, and the average difference being only 275 ppm. If the $^{87}Sr/^{86}Sr$ in these sills has been affected by alteration, the process has affected both sills (and all samples) in a very similar way, and the alteration has been so pervasive that the leachable and unleachable $^{87}Sr/^{86}Sr$ is not distinguishable. While it would be reckless to draw apodictic conclusions from these highly altered sills, the most parsimonious interpretation is that the $^{87}Sr/^{86}Sr$ ratios are close to primary magmatic values.

Fig. 10 shows the model present-day isotope data for Sr, Nd and Pb. First, it is clear from the Nd and Pb isotope data that the upper and lower sills are not strictly co-genetic, but have distinctly different isotopic signatures. It is also clear (as with the trace elements) that the sills are not even remotely MORB-like, so are not related to normal ocean crust production from the depleted upper mantle. In comparison with a sampling of isotopic data from North Atlantic hotspot basalts (Iceland, Azores, Canaries, Madeira), the Pb isotope arrays fall close to the hotspot fields, but with a clear divergence toward higher $^{207}Pb/^{204}Pb$ at lower $^{206}Pb/^{204}Pb$; this is a hallmark of both the oceanic EM1 mantle end-member, and of old continental lithosphere. This divergence is even more obvious in the Nd-Pb isotope plot, where the data for the Site 1276 sills ranges orthogonally away from the field of North Atlantic hotspots. The mixing end-member for this array is very similar to the EM1 hotspot mantle end-member (though the closest such hotspot is Gough Island, S. Atlantic!). In Nd-Sr isotope space, the sill data fall at the high $^{87}Sr/^{86}Sr$ end of the North Atlantic hotspot field – but well within the domain of EM2 hotspots (e.g. Samoa or the Societies). Our conclusion is that the sills are clearly not MORB-like, but fall within the general global domain of plumes or hotspots, though none of the known North Atlantic "plumes" are a close match to the sills. As yet, the nearest hotspots (Newfoundland and Milne Seamounts) are isotopically *incognitus* in the published literature.

## Summary

The Site 1276 basaltic sills were intruded into a significant overburden of syn-rift sediments, and are some 25 Ma younger than the underlying basement. Their enriched geochemistry identifies them as likely being of hotspot or plume derivation, but they are definitely not of MORB spreading ridge character. Several scenarios are possible: 1). The sills were intruded off-axis through typical MORB ocean crust, several hundred km west of an active spreading center. Their alkaline character reflects preferential melting of enriched enclaves embedded in depleted MORB mantle (similar to the model proposed by Zindler et al. (1984) and Castillo and Batiza (1989) for off-axis EPR and MAR seamounts). 2). The sills, and the older underlying basement, are both of alkaline character, formed from plume-type mantle during the transitional stages of rifting. The Milne Seamount chain to the east may be implicated in this magmatism. Thus the enduring enigma of early-rift magmatism persists, and a final resolution must await a full penetration to basement at a drill site such as Site 1276.

## Acknowledgments

We thank Brian Tucholke for piquing our interest in Site 1276, and for his helpful tutorials on same. Lary Ball performed his usual miracles with the NEPTUNE. Matt Jackson carried out the electron probe work and did the Ba sleuthing. Helpful reviews were provided by Stephanie Ingle and Georgia Pe-Piper. This research used samples provided by the Ocean Drilling Program (ODP is sponsored by the U.S. National Science Foundation (NSF) and participating countries under management of Joint Oceanographic Institutions (JOI), Inc.). Funding for this research was provided by JOI/USSSP 261855 and NSF-EAR0509891.

## References

Abouchami, W., Galer, S. J. G., Koschinsky, A., 1999. Pb and Nd isotopes in NE Atlantic Fe-Mn crusts: proxies for trace metal paleosources and paleocean circulation. Geochim. Cosmochim. Acta 63, 1489-1505.

Castillo, P. and Batiza, R., 1989. Strontium, neodymium and lead isotope constraints on near-ridge seamount production beneath the South Atlantic. Nature 342, 262-265.

Cheng, Q., Park, K.-H., Macdougall, J. D., Zindler, A., Lugmair, G. W., Hawkins, J. Lonsdale, P. and Staudigel, H., 1987. Isotopic evidence for a hot spot origin of the Louisville seamount

chain. In: Seamounts, Islands and Atolls, B. Keating, P. Fryer, R. Batiza and G. W. Boehlert, eds., Am. Geophys. Union Monogr. 43, 283-296.

Cotten J., Le Dez, A., Bau, M., Caroff, M., Maury, R. C., Dulski, P., Fourcade, S., Bohn, M., Brousse, R., 1995. Origin of anomalous rare-earth element and Yttrium enrichments in subaerially exposed basalts: Evidence from French Polynesia. Chemical Geology 119, 115-138.

Dick, H. J. B. and Johnson K. T. M., 1995. REE and Trace Element Composition of Clinopyroxene Megacrysts, Xenocrysts, and Phenocrysts in Two Diabase Dikes from Leg 140, Hole 504B. Proc. ODP 137/140, 121-130.

Duncan, R. A. and Keller, R. A., 2004. Radiometric ages for basement rocks from the Emperor Seamounts, ODP Leg 197. Geochemistry, Geophysics, Geosystems 5(8): Q08L03, doi:10.1029/2004GC000704.

Eisele, J., Sharma, M., Galer, S.J.G., Blichert-Toft, J., Devey, C.W., Hofmann, A.W., 2002. The role of sediment recycling in EM-1 inferred from Os, Pb, Hf, Nd, Sr isotope and trace element systematics of the Pitcairn hotspot. Earth and Planetary Science Letters,196, 197-212.

Fodor R. V., Malta, D. P., Bauer, G. R., Jacobs, R. S., 1989. Microbeam Analyses of Rare-Earth Element Phosphate in Basalt from Kahoolawe Island, Hawaii. In: Proceedings of the 24th Annual Conference of the Microbeam Analytical Society, 554-558.

Galer, S. J. G., 1986. Chemical and isotopic studies of crust-mantle differentiation and the generation of mantle heterogeneity. Unpubl. PhD., University of Cambridge.

Gao, S., Luo, T-C., Zhang, B-R., Zhang, H-F., Han, Y-W., Zhao, Z-D., Hu, Y-K., 1998. Chemical composition of the continental crust as revealed by studies in East China. Geochimica et Cosmochimica Acta 62, 1959-1975.

Hart, S.R. and Gaetani, G.A., 2006. Mantle Pb paradoxes: the sulfide solution. Contributions to Mineralogy and Petrology 152, xxx.

Hart, S. R., Workman, R. K., Coetzee, M., Blusztajn, J., Ball, L., Johnson, K. T. M., 2002. The Pb Isotope Pedigree of Western Samoan Volcanics: New Insights from High-Precision Analysis by NEPTUNE ICP/MS, EOS 83, F20.

Hart, S. R., Ball, L., and Jackson, M., 2005. Sr Isotopes by Laser Ablation PIMMS: Application to Cpx from Samoan Peridotite Xenoliths, *WHOI Plasma Facility Open File Technical Report 11*. (http://www.whoi.edu/science/GG/people/shart/open_file.htm)

Hart, S. R., Workman, R. K., Ball, L., and Blusztajn, J., 2004. High Precision Pb Isotope Techniques from the WHOI NEPTUNE PIMMS, *WHOI Plasma Facility Open File Technical Report 10*. (http://www.whoi.edu/science/GG/people/shart/open_file.htm)

Hauri, E.H. and Hart, S.R., 1997. Rhenium abundances and systematics in oceanic basalts. Chemical

Geology 139,185-205.

Hawkesworth, C.J., Gallagher, K., Kirstein, L., Montovani, M.S.M., Peate, D.W., and Turner, S.P., 2000. Tectonic controls on magmatism associated with continental break-up: an example from the Paraná-Etendeka Province. Earth and Planetary Science Letters 179, 335-349.

Hawkesworth, C.J., Kelley, S., Turner, S.P., le Roex, A., and Storey, B., 1999. Mantle processes during Gondwana breakup and dispersal. J. Afr. Earth Sci. 28, 239-261.

Hofmann, A., 2003. Sampling Mantle Heterogeneity through Oceanic Basalts: Isotopes and Trace Elements. In: H.D. Holland and K. K. (Editors), Treatise on Geochemistry, 2.03, 61-101.

Hofmann, A.W. and White, W.M., 1983. Ba, Rb and Cs in the Earth's Mantle. Z. Naturforsch 38a, 256-266.

Hopper, J.R., Funck, T., Tucholke, B.E., Larsen, H.C., Holbrook, W.S., Louden, K.E., Shillington, D.J., and Lau, H., 2004. Continental breakup and the onset of ultraslow seafloor spreading off Flemish Cap on the Newfoundland rifted margin. Geology 32, 93-96.

Hurtubise, D.O., Puffer, J.H., and Cousminer, H.L., 1987. An offshore Mesozoic igneous sequence, Georges Bank basin, North Atlantic. Geological Society of America Bulletin 98, 430-438.

Jackson, M. G. and S. R. Hart, 2006. Strontium Isotopes in melt inclusions from Samoan basalts: Implications for the heterogeneity in the Samoan plume. Earth and Planetary Science Letters 245, 260-277.

Jansa, L.F., and Pe-Piper, G., 1988. Middle Jurassic to Early Cretaceous Igneous Rocks Along Eastern North American Continental Margin. American Association of Petroleum Geologists Bulletin 72, 347-366.

Johnson, D.M., Hooper, P.R., Conrey, R.M., 1999. XRF Analysis of Rocks and Minerals for Major and Trace Elements in a Single Low Dilution Li-tetraborate Fused Bead. Advances in X-Ray Analysis 41, 843-867.

Karner, G.D., and Shillington, D.J., 2005. Basalt sills of the U reflector, Newfoundland Basin: A serendipitous dating technique. Geology 33, 985-988.

Keen, C. E., Courtney, R. C., Dehler, S. A., Williamson, M.-C., 1994. Decompression melting at rifted margins: comparison of model predictions with the distribution of igneous rocks on the eastern Canadian margin. Earth and Planetary Letters 121, 403-416.

King, S.D., and Anderson, D.L., 1998. Edge-driven convection. Earth and Planetary Science Letters 160, 289-296.

Knaack, C.M., Cornelius, S.B., Hooper, P.R., 1994. Trace element Analysis of rocks and minerals by ICP-MS. In: Open File Report, GeoAnalytical Lab, Washington State University, p. 10.

Koppers, A.A.P., Staudigel, H., Duncan, R.A., 2003. High-Resolution $^{40}Ar/^{39}Ar$ dating of the oldest oceanic basement basalts in the western Pacific basin. Geochemistry, Geophysics, Geosystems 4(11):8914, doi:8910.1029/2003GC000574.

Leitch, A. M., Davies, G. F., Wells, M., 1998. A plume head melting under a rifting margin, Earth and Planetary Science Letters 161, 161-177.

Mahoney, J. J., 1987. An isotopic survey of Pacific oceanic plateaus: implications for their nature and origin, in: Keating, B. H., Fryer, P., Batiza, R. and Boehlert, G. W. (eds), Seamounts, Islands and Atolls, Am. Geophys. Union Monogr. 42, 207-220.

McCulloch, M.T., Bennett, V.C., 1994. Progressive growth of the Earth's continental crust and depleted mantle. Geochimica et Cosmochimica Acta 58, 4717-4738.

McDonough, W.F., and Sun, S-s, 1995. The composition of the Earth. Chemical Geology 120, 223-253.

McHone, J.G., 1992. Mafic dike suites within Mesozoic igneous provinces of New England and Atlantic Canada, p. 1-11 *in*: Eastern North American Mesozoic Magmatism, , Puffer, J.H., and Ragland, P.C., eds., Geological Society of America Special Paper 268, 406 p.

Morris, J.D. and Hart, S.R., 1983. Isotopic and incompatible element constraints on the genesis of island arc volcanics from Cold Bay and Amak Island, Aleutians, and implications for mantle structure. Geochim. Cosmochim. Acta 47, 2015-2030.

Mutter, J.C., 1993. Margins declassified. Nature 364, 393–394.

Mutter, J.C., Buck, W.R., and Zehnder, C.M., 1988. Convective partial melting, 1. A model for the formation of thick basaltic sequences during the initiation of spreading. J. Geophys. Res. 93, 1031–1048.

Pan, Y. and Batiza, R., 2003. Magmatic processes under mid-ocean ridges: A detailed mineralogic study of lavas from East Pacific Rise 9°30'N 10°30'N and 11°20'N. Geochemistry, Geophysics, Geosystems, 4(11) 8623, doi:10.1029/2003GC000309.

Pegram, W. J., 1990. Development of continental lithospheric mantle as reflected in the chemistry of the Mesozoic Appalachian tholeiites, U. S. A. Earth Planetary Science Letters 97, 316-331.

Pe-Piper, G., Jansa, L.F., Palacz, Z. 1994. Geochemistry and regional significance of the Early Cretaceous bimodal basalt-felsic associations on the Grand Banks, eastern Canada. Geological Society of America Bulletin 106, 1319-1331.

Pe-Piper, G., and Jansa, L.F., 1987. Geochemistry of the late Middle Jurassic—Early Cretaceous igneous rocks on the eastern North American margin. Geological Society of America Bulletin 99, 803-813.

Pe-Piper, G., Jansa, L.F., and Lambert, R.S.J., 1992. Early Mesozoic magmatism on the Eastern Canadian margin: Petrogenic and tectonic significance, p. 13-36 i*n*: Eastern North American Mesozoic Magmatism, , Puffer, J.H., and Ragland, P.C., eds., Geological Society of America Special Paper 268, 406 p.

Pe-Piper, G., Piper, D.J.W., Keen, M.J., and McMillan, N.J., 1990. Igneous rocks of the continental margin: tectonic and geophysical overview. p.75-84 *in*: Keen, M.J., and Williams, G.L., Eds., Geology of the Continental Margin of Eastern Canada. Geol. Soc. Am. Memoir 2, 855 p.

Plank, T., and Langmuir, C.H., 1998. The chemical compositions of subducting sediments and its consequences for the crust and mantle. Chemical Geology 145, 325-394.

Rohrman, M., and van der Beek, P., 1996. Cenozoic postrift domal uplift of North Atlantic margins: An asthenospheric diapirism model. Geology 24, 901-904.

Ross, M.E., 1992, Petrology and tectonic significance of Mesozoic mafic dikes of the coastal New England igneous province, Massachusetts. *in* Puffer, J.H., and Ragland, P.C., eds., Eastern North American Mesozoic Magmatism. Geological Society of America Special Paper 268, 406 p.

Rudnick, R.L., Fountain, D.M., 1995. Nature and composition of the continental crust: a lower crustal perspective. Review of Geophysics 33, 267-309.

Shipboard Scientific Party, 2004. Leg 210 summary, In: Tucholke, B.E., Sibuet, J.-C., Klaus, A., et al., Proc. ODP Init. Repts., 210: College Station TX (Ocean Drilling Program), 1–78.

Su, Y., and Langmuir, C. H., 2003, Global MORB chemistry compilation at the segment scale, MS Thesis, Department of Earth and Environmental Sciences, Columbia University. Available at: http://petdb.ldeo.columbia.edu/documentation/morbcompilation/.

Sullivan, K. D. and Keen, C. E., 1977. Newfoundland Seamounts – Petrology and Geochemistry, *in* Baragar, W.R.A., Coleman, L.C., Hall, J.M., eds., Volcanic regimes of Canada, Geol. Assoc. Canada Special Paper 16, 461-476.

Taras, B. D., Hart, S.R., 1987. Geochemical evolution of the New England seamount chain: isotopic and trace element constraints. Chemical Geology 64, 35-54.

Tucholke, B.E., Sibuet, J.-C., Klaus, A., et al., 2004. Proc. ODP, Init. Repts., 210. Ocean Drilling Program, College Station TX.

Todt, W., Cliff, R.A., Hanser, A., Hofmann, A. W., 1996. Evaluation of a 202Pb-205Pb double spike for high-precision lead isotope analysis, I*n*: Basu, A. and Hart, S.R., (Eds.) Earth

Processes: Reading the Isotopic Code. Am. Geophys. Union Geophysical Monograph 95, 429-437.

White, R.S., and McKenzie, D., 1989. Magmatism at rift zones: the generation of volcanic continental margins and flood basalts. J. Geophys. Res. 94, 7685–7729.

White, R.S., Spence, G.D., Fowler, S.R., McKenzie, D.P., Westbrook, G.K., and Bowen, A.N., 1987. Magmatism at rifted continental margins. Nature 330, 439–444.

Woodhead J.D., 1996. Extreme HIMU in an oceanic setting: the geochemistry of Mangaia Island (Polynesia), and temporal evolution of the Cook-Austral hotspot. J. Volcanology and Geothermal Research 72, 1-19.

Workman, R. K., Hart, S. R., Jackson, M., Regelous, M, Blusztajn, J., Kurz, M., Farley, K., and Staudigel, H., 2004. Recycled Metasomatized Lithosphere as the Origin of the Enriched Mantle II (EM2) End-member: Evidence from the Samoan Volcanic Chain. G-Cubed 5, 2003GC000623.

Zindler, A., Staudigel, H., and Batiza, R., 1984. Isotope and trace element geochemistry of young Pacific seamounts: implications for the scale of upper mantle heterogeneity. Earth and Planetary Science Letters 70, 175-195.

**Figure Captions**

Fig. 1. Bathymetry of the northern Newfoundland Basin, showing the location of Site 1276 at the foot of the continental rise south of Flemish Cap. The Newfoundland and Milne seamount chains are also shown. Site 1276 was drilled in 4560 m of water, to a total depth of 1739 m below sea floor, at 45° 24.3198'N, 44° 47.1496'W.

Fig. 2. Alkali-Silica classification plot showing that both lower (blue diamonds) and upper (red circles) sills from Site 1276 lie in the hawaiite field. A global average (Su and Langmuir, 2003) of normal mid-ocean ridge basalts (N-MORB, filled square) lies well below the alkali basalt-tholeiite dividing line. Data are for unleached powders; Table 2.

Fig. 3. $Al_2O_3$-$TiO_2$ contents of clinopyroxenes from two samples, Site 1276 sills. Data for the clinopyroxene compositions is given in Table 1, Supplementary material. Representative N-MORB clinopyroxene compositions are from Dick and Johnson (1995) and Pan and Batiza (2003).

Fig. 4. $Na_2O$, Ba and volatile content of lower (blue diamonds) and upper (red circles) sills from Site 1276. Note log scale for Ba, and the general correlation of high Ba and low $Na_2O$ with increasing alteration (high volatile content). Data are for unleached powders; Table 2.

Fig. 5. Trace element abundances (spidergram) for the ratio of concentration in leached rock powder divided by concentration in unleached rock powder (Table 2); average of three upper sill samples – red circles; average of three lower sill samples – blue diamonds.

Fig. 6. $^{40}Ar/^{39}Ar$ stepwise heating profiles for two un-leached upper sill samples (88-2, 88-3) and two un-leached lower sill samples (99-3, 99-6). Data for these ages is given in Table 2, Supplementary material. Step-release heating from 500°-1400°C; 2-sigma errors include measurement uncertainties, and uncertainty in J-value (flux gradient from FCT-3 biotite monitor), but not uncertainty in monitor age. Ages determined in Bob Duncan's Noble Gas Mass Spectrometry Lab, Oregon State University. Details of the techniques are given in Duncan and Keller, 2004, and Koppers et al., 2003.

Fig. 7. Trace element abundances for the average of three upper sill (red circles) and three lower sill (blue diamonds) samples, normalized to bulk silicate earth abundances (McDonough and Sun, 1995; Cs value was adjusted down to 0.010 ppm to provide a more realistic Rb/Cs = 60 for BSE). An average EM2 basalt pattern, dashed line, is shown for comparison (average of 5 highest $^{87}Sr/^{86}Sr$ basalts from Malumalu seamount, Samoa; Workman et al., 2004). Data are for un-leached powders; Table 2.

Fig. 8. La/Sm-Nb/Nb* for Site 1276 sills (lower sill - shaded diamonds, upper sill – shaded circles. Data are for unleached powders; Table 2), in comparison with various estimates of continental crust (red squares), and the mantle end-members N-MORB, EM1, EM2 and HIMU (yellow triangles): (Continental crust estimates - Rudnick and Fountain, 1995, McCulloch and Bennett, 1994, Gao et al., 1998, Plank and Langmuir, 1998. HIMU – average of 21 samples from Mangaia and Tubuai Islands: Woodhead, 1996; Hauri and Hart, 1997. EM1 – average of 18 samples of Tedside Series, Pitcairn Island: Eisele et al., 2002; Hauri, Hart and Farley, unpublished. EM2 – average of 6 samples from Malumalu seamount, Samoa: Workman et al., 2004. N-MORB – global average of Su and Langmuir, 2003. Nb/Nb* = (Nb)n/[(Th)n*(La)n]^0.5.

Fig. 9. Zr, Ba and Sr contents of the Site 1276 sills (shaded circles – upper sill; shaded diamonds

– lower sill. Data are for unleached powders; Table 2) in comparison to: N-MORB (filled triangle), Mesozoic Appalachian Tholeiites (MAT, open circle) and other mafic rift-related volcanics from the Newfoundland Seamounts (small open squares) and Grand Banks, Scotia Shelf, NE Seamounts, Georges Bank, Baltimore Canyon, and average lamprophyres from New England and Quebec (shaded squares); Data from Hurtibise et al.,1987; McHone, 1992; Pegram, 1990; Pe-Piper and Jansa, 1987; Pe-Piper et al., 1990, 1992, 1994; Ross, 1992; Sullivan and Keen, 1977.

Fig. 10. Sr, Nd and Pb isotope ratios of Site 1276 sills (upper sill-large shaded circles; lower sill-large shaded diamonds) compared with North Atlantic MORB (small circles; PETDB data base) and basalts from North Atlantic hotspots/plumes (Azores, Canaries, Iceland, Madeira; GEOROC Data Base). Sill data are for leached powders, Table 2, corrected back to initial ratios and forward to present using a mantle evolution model; see text and Table 3.

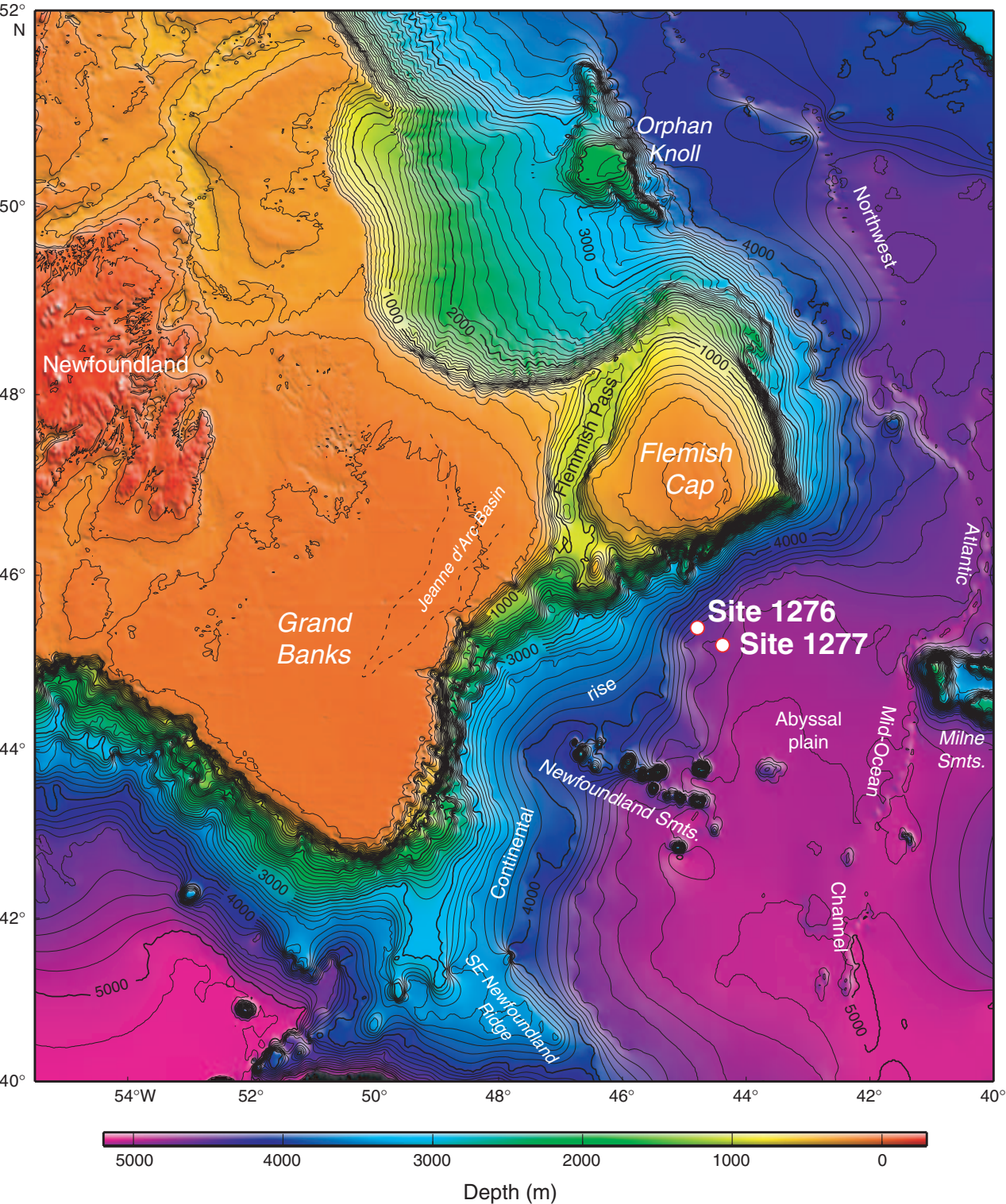
52° N
50°
48°
46°
44°
42°
40°
54°W
52°
50°
48°
46°
44°
42°
40°
Orphan Knoll
Northwest
Newfoundland
Flemish Pass
Flemish Cap
Jeanne d'Arc Basin
Grand Banks
Site 1276
Site 1277
Atlantic
rise
Abyssal plain
Mid-Ocean
Milne Smts.
Newfoundland Smts.
Continental
Channel
SE Newfoundland Ridge
5000
4000
3000
2000
1000
0
Depth (m)

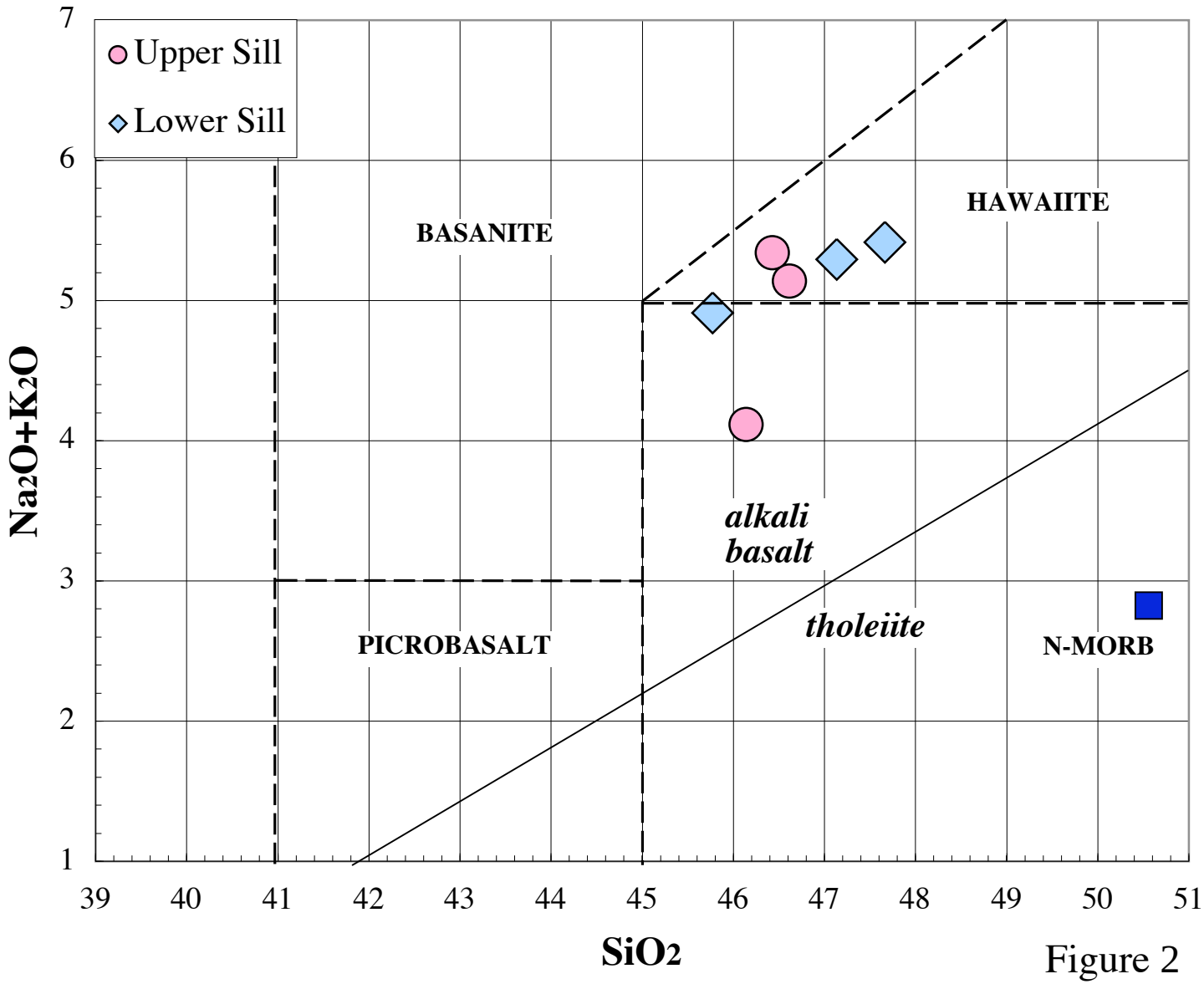
Upper Sill
Lower Sill
BASANITE
HAWAIITE
alkali basalt
tholeiite
PICROBASALT
N-MORB
Na2O+K2O
SiO2
7
6
5
4
3
2
1
39
40
41
42
43
44
45
46
47
48
49
50
51

Figure 2

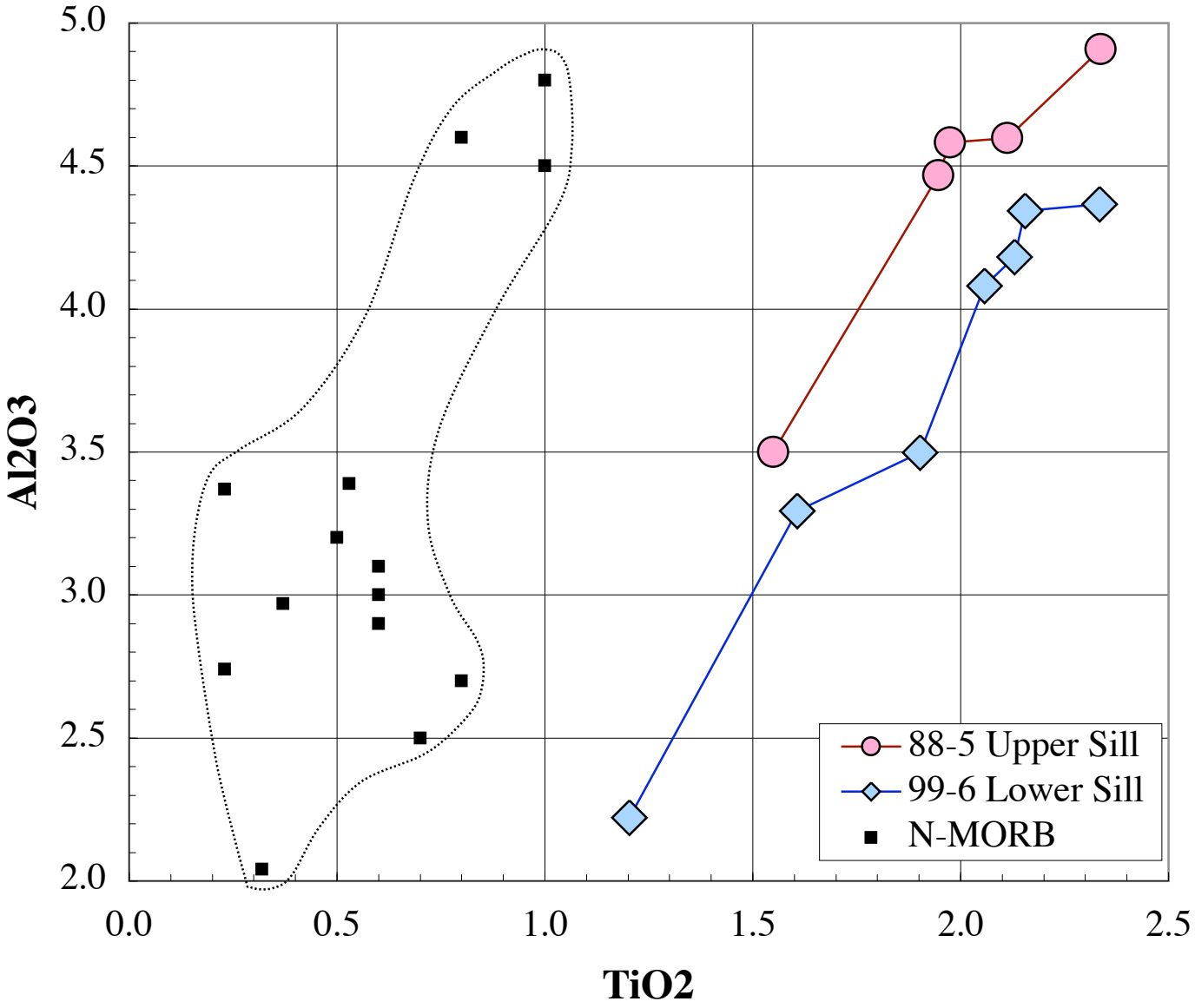
5.0
4.5
4.0
3.5
3.0
2.5
2.0
Al2O3
0.0
0.5
1.0
1.5
2.0
2.5
TiO2
88-5 Upper Sill
99-6 Lower Sill
N-MORB

Figure 3

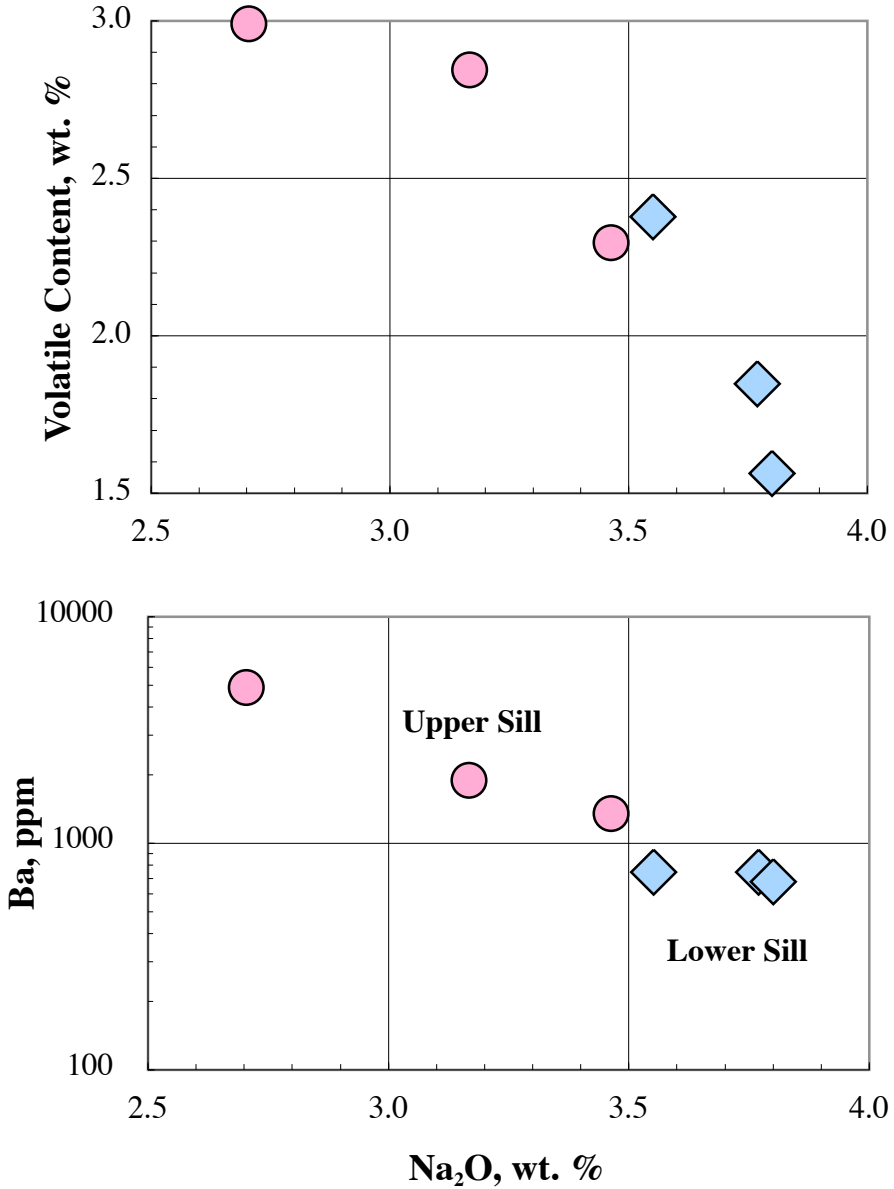
3.0
2.5
2.0
1.5
Volatile Content, wt. %
2.5
3.0
3.5
4.0
10000
1000
100
Ba, ppm
Upper Sill
Lower Sill
2.5
3.0
3.5
4.0
Na2O, wt. %

**Figure 4**

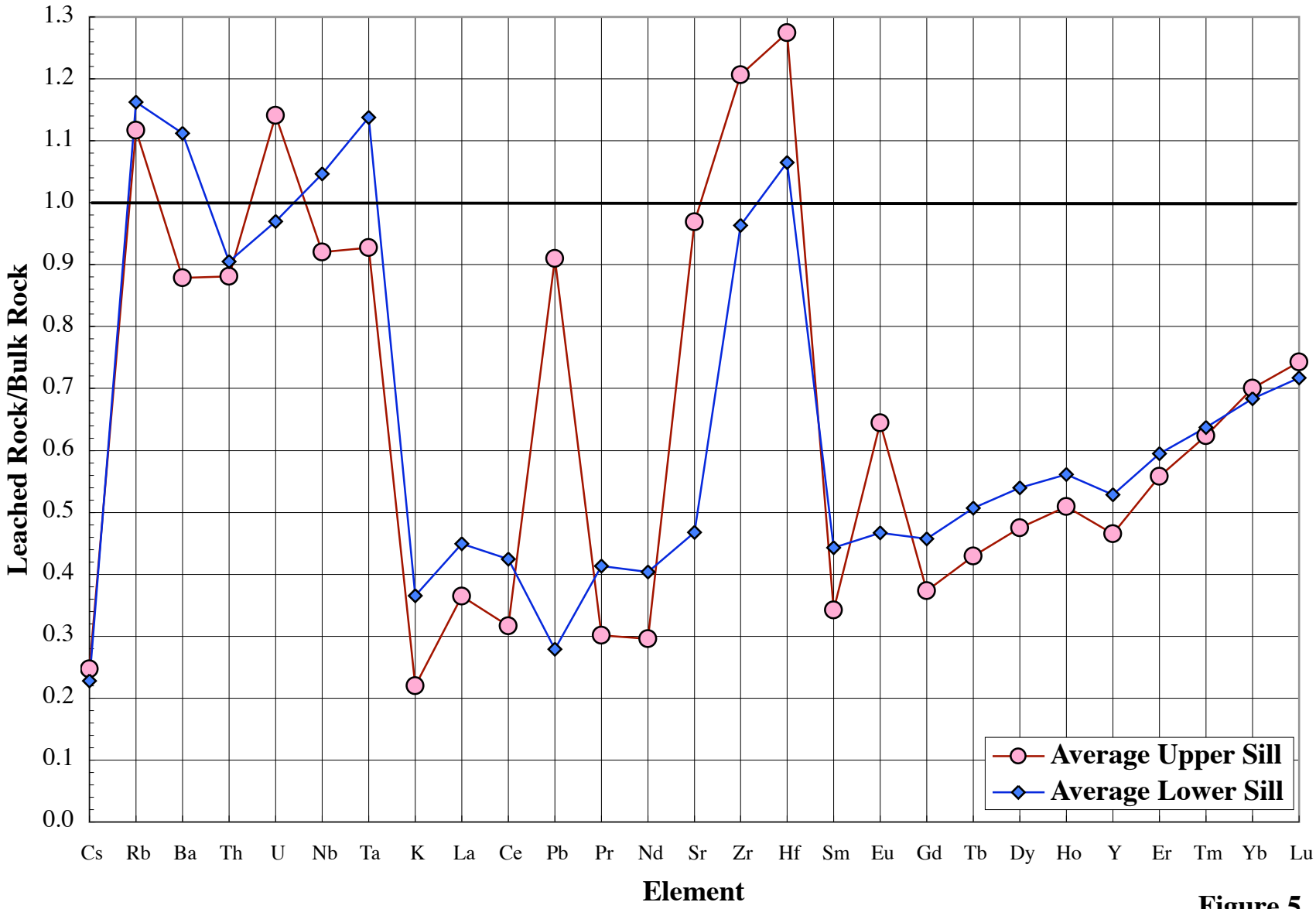
Leached Rock/Bulk Rock
1.3
1.2
1.1
1.0
0.9
0.8
0.7
0.6
0.5
0.4
0.3
0.2
0.1
0.0
Cs Rb Ba Th U Nb Ta K La Ce Pb Pr Nd Sr Zr Hf Sm Eu Gd Tb Dy Ho Y Er Tm Yb Lu
Element
Average Upper Sill
Average Lower Sill

**Figure 5**

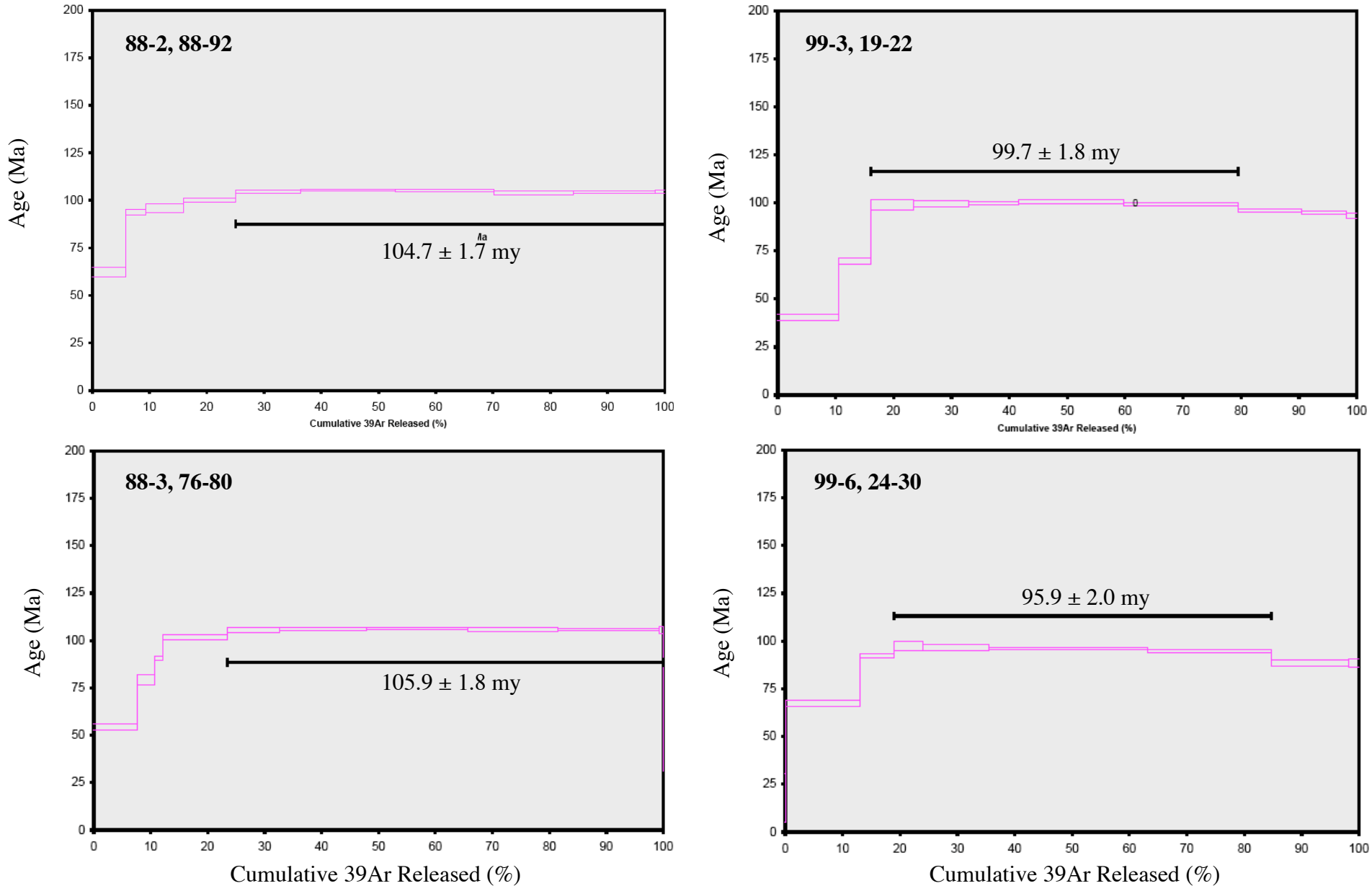
88-2, 88-92
104.7 ± 1.7 my
99-3, 19-22
99.7 ± 1.8 my
88-3, 76-80
105.9 ± 1.8 my
99-6, 24-30
95.9 ± 2.0 my
Age (Ma)
Cumulative 39Ar Released (%)

**Figure 6**

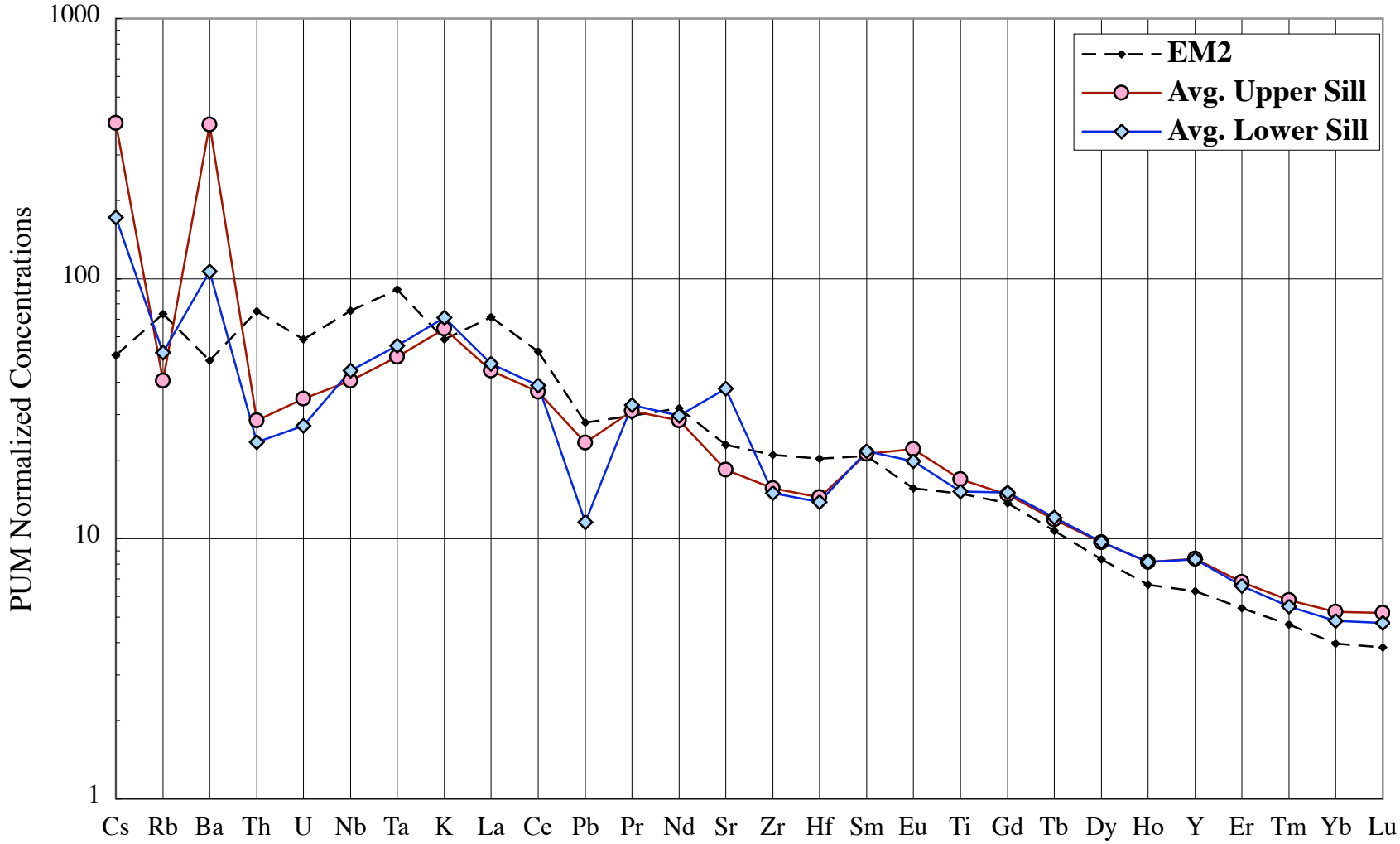
1000
100
10
1
PUM Normalized Concentrations
EM2
Avg. Upper Sill
Avg. Lower Sill
Cs Rb Ba Th U Nb Ta K La Ce Pb Pr Nd Sr Zr Hf Sm Eu Ti Gd Tb Dy Ho Y Er Tm Yb Lu

**Figure 7**

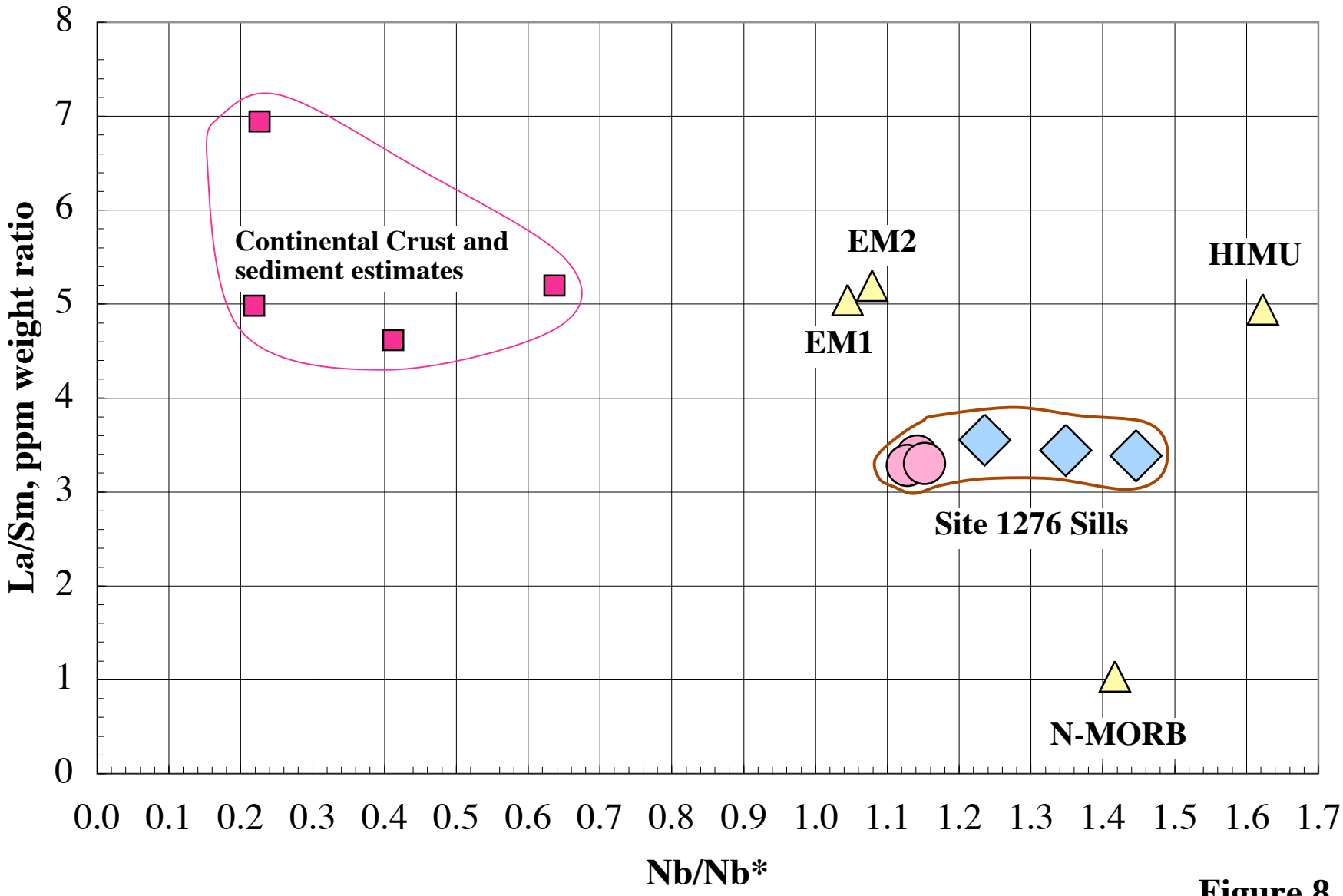
La/Sm, ppm weight ratio
Nb/Nb*
0
1
2
3
4
5
6
7
8
0.0
0.1
0.2
0.3
0.4
0.5
0.6
0.7
0.8
0.9
1.0
1.1
1.2
1.3
1.4
1.5
1.6
1.7
Continental Crust and sediment estimates
EM2
EM1
HIMU
Site 1276 Sills
N-MORB

**Figure 8**

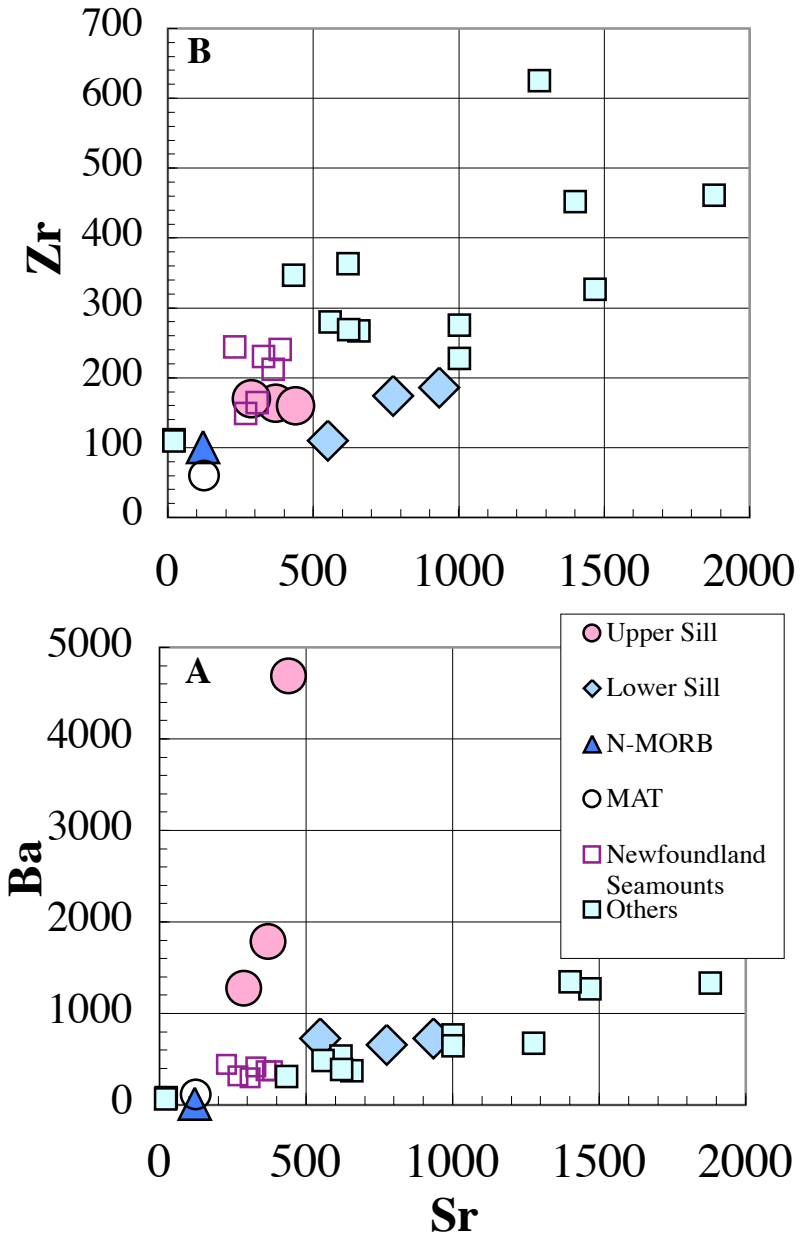
B
Zr
700
600
500
400
300
200
100
0
0
500
1000
1500
2000
A
Ba
5000
4000
3000
2000
1000
0
0
500
1000
1500
2000
Sr
Upper Sill
Lower Sill
N-MORB
MAT
Newfoundland Seamounts
Others

**Figure 9**

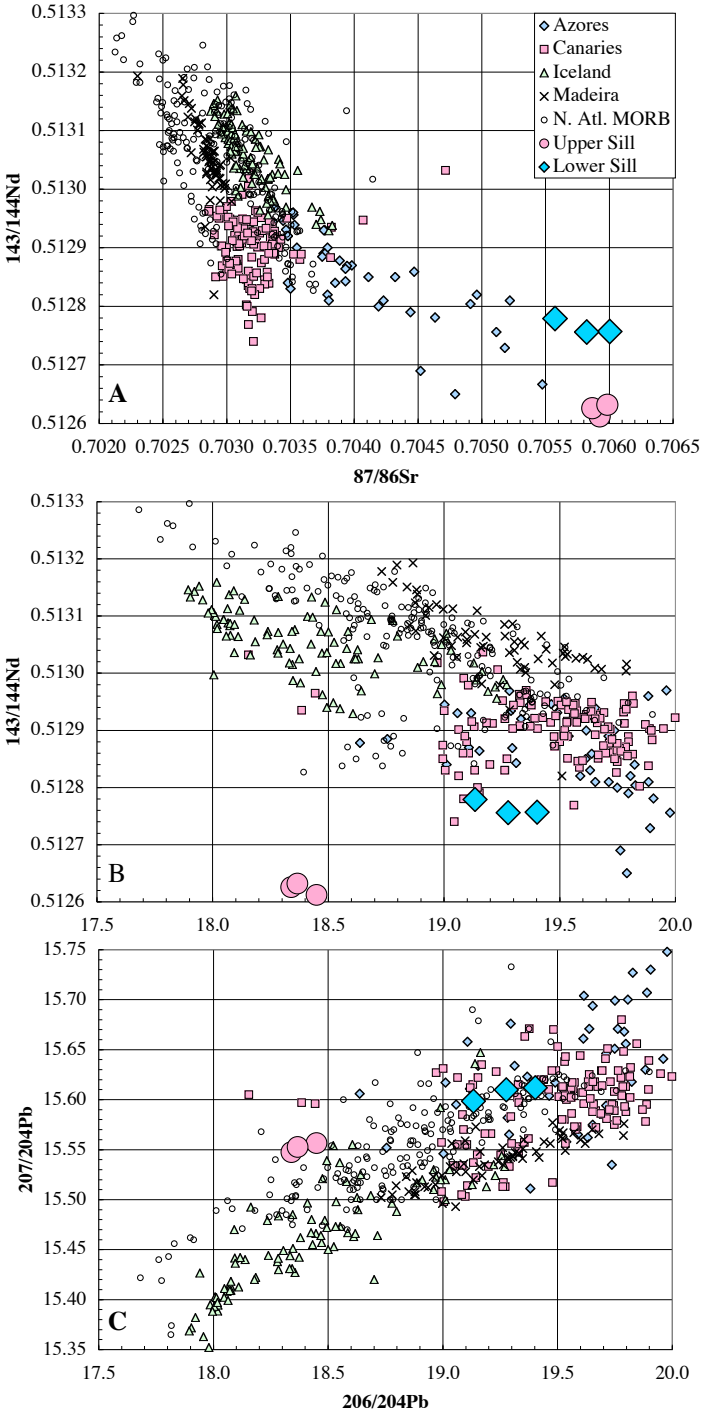
Azores
Canaries
Iceland
Madeira
N. Atl. MORB
Upper Sill
Lower Sill
A
B
C
143/144Nd
87/86Sr
207/204Pb
206/204Pb
0.5133
0.5132
0.5131
0.5130
0.5129
0.5128
0.5127
0.5126
0.7020 0.7025 0.7030 0.7035 0.7040 0.7045 0.7050 0.7055 0.7060 0.7065
17.5 18.0 18.5 19.0 19.5 20.0
15.75
15.70
15.65
15.60
15.55
15.50
15.45
15.40
15.35

Figure 10

## Table 1 - Leg 210 Site 1276 Sample Inventory and Petrographic Notes

| Site | Core | Section | Piece Depth cm | Mid-interval Depth mbsf | Weight grams | Alteration | Grain Size | Comments |
|---|---|---|---|---|---|---|---|---|
| Upper contact | | | | 1612.83 | - | | | |
| 1276 | 87 | 6 | 102-104 | 1613.14 | 31 | high | fine | up to 5% apatite, abundant carbonate |
| 1276 | 88 | 1 | 83-86 | 1614.95 | 48 | moderate to high | fine | Moderate clay and carbonate, some apatite |
| 1276 | **88** | **2** | 88-92 | 1616.02 | 59 | moderate | fine | Some carbonate patches, trace of apatite and biotite |
| 1276 | 88 | 3 | 29-33 | 1616.87 | 50 | high | fine | Abundant clay, carbonate and apatite |
| 1276 | 88 | 3 | 48-51 | 1617.06 | 49 | moderate | fine | Some oxide exsolution, little carbonate or apatite. |
| 1276 | **88** | **3** | 76-80 | 1617.34 | 54 | moderate to low | fine | Clean plagioclase and oxides, 20% clay, rare carbonate; best of core 88 |
| 1276 | 88 | 4 | 39-41 | 1618.46 | 63 | moderate | fine | Clean plagioclase and oxides, 25% clay, some apatite and biotite |
| 1276 | **88** | **5** | 67-71 | 1620.22 | 51 | moderate | fine | Clean plagioclase and oxides, 25% clay, 3% apatite and some biotite |
| 1276 | 88 | 6 | 48-51 | 1621.12 | 57 | moderate | aphanitic | Abundant clean cpx and oxides, 25% clay, some carbonate |
| 1276 | 88 | 7 | 81-85 | 1622.66 | 51 | high | aphanitic | Abundant clay and carbonate, exsolved oxides |
| Lower contact | | | | 1623.00 | - | | | |
| Upper contact not recovered | | | | <1715.33 | - | | | |
| 1276 | 99 | 1 | 46-49 | 1719.88 | 39 | moderate to high | fine | Some oxide exsolution, very altered groundmass |
| 1276 | 99 | 2 | 0-4 | 1720.85 | 42 | moderate | fine | 20% large clean cpx phenocrysts, altered plagioclase, minimal carbonate |
| 1276 | **99** | **3** | 19-22 | 1722.49 | 47 | moderate to low | medium | 35% large clean cpx phenocrysts, minimal carbonate; best of core 99 |
| 1276 | 99 | 5* | 10-13 | 1724.07 | 47 | moderate | medium | 30% large clean cpx phenocrysts, minimal carbonate, altered groundmass |
| 1276 | **99** | **5*** | 30-34 | 1724.28 | 61 | moderate | medium | 25% large clean cpx phenocrysts, minimal carbonate, altered groundmass |
| 1276 | **99** | **6*** | 24-27 | 1725.42 | 62 | moderate | medium | 25% large clean cpx phenocrysts, minimal carbonate, altered groundmass |
| 1276 | **99** | **6*** | 27-30 | 1725.44 | 58 | moderate | medium | 25% large clean cpx phenocrysts, minimal carbonate, altered groundmass |
| Lower contact not recovered | | | | >1725.59 | - | | | |

* Section out of order & pieces may not be in correct order
Samples with Core and Section in Bold font were used for chemical and isotopic analysis (the two 99-6 samples were combined)
Site 1276 was drilled to a depth of 1739m bsf in 4560m water depth at 45° 24.3198'N, 44° 47.1496' W.

**Table 2. Chemical and isotopic data for leached and unleached volcanics, Site 1276, ODP Leg 210**

| | 88-2 | 88-2L | 88-3 | 88-3L | 88-5 | 88-5L | 99-3 | 99-3L | 99-5 | 99-5L | 99-6 | 99-6L |
|---|---|---|---|---|---|---|---|---|---|---|---|---|
| **SiO2** | 46.62 | | 46.43 | | 46.14 | | 45.77 | | 47.67 | | 47.14 | |
| **TiO2** | 3.544 | | 3.478 | | 3.531 | | 3.612 | | 3.465 | | 3.591 | |
| **Al2O3** | 15.33 | | 14.92 | | 14.68 | | 14.87 | | 15.38 | | 15.18 | |
| **FeO*** | 14.65 | | 14.56 | | 14.73 | | 15.42 | | 13.32 | | 14.29 | |
| **MnO** | 0.320 | | 0.347 | | 0.331 | | 0.236 | | 0.201 | | 0.205 | |
| **MgO** | 8.06 | | 7.84 | | 8.30 | | 6.12 | | 4.87 | | 5.15 | |
| **CaO** | 5.63 | | 6.38 | | 7.50 | | 8.52 | | 9.14 | | 8.60 | |
| **Na2O** | 3.17 | | 3.46 | | 2.70 | | 3.55 | | 3.77 | | 3.80 | |
| **K2O** | 1.970 | 0.382 | 1.875 | 0.365 | 1.408 | 0.382 | 1.360 | 0.617 | 1.648 | 0.436 | 1.493 | 0.563 |
| **P2O5** | 0.708 | | 0.700 | | 0.672 | | 0.538 | | 0.535 | | 0.550 | |
| **Sum** | 100.00 | | 100.00 | | 100.00 | | 100.00 | | 100.00 | | 100.00 | |
| **Raw Sum** | 97.16 | | 97.70 | | 97.01 | | 97.62 | | 98.15 | | 98.44 | |
| **XRF Trace Elements (ppm)** | | | | | | | | | | | | |
| **Ni** | 26.0 | | 30.9 | | 35.9 | | 53.3 | | 28.6 | | 36.3 | |
| **Cr** | 32.6 | | 42.7 | | 52.2 | | 45.3 | | 9.0 | | 17.3 | |
| **Sc** | 27.3 | | 26.9 | | 28.6 | | 26.7 | | 27.2 | | 26.3 | |
| **V** | 360 | | 355 | | 375 | | 408 | | 363 | | 383 | |
| **Ba** | 1887 | | 1345 | | 4855 | | 748 | | 744 | | 678 | |
| **Rb** | 28.8 | | 28.0 | | 21.9 | | 31.6 | | 36.0 | | 32.8 | |
| **Sr** | 387 | | 294 | | 440 | | 558 | | 912 | | 756 | |
| **Zr** | 180 | | 186 | | 176 | | 229 | | 242 | | 240 | |
| **Y** | 30.8 | | 31.7 | | 29.7 | | 32.1 | | 32.2 | | 32.0 | |
| **Nb** | 28.0 | | 28.7 | | 27.6 | | 28.0 | | 29.8 | | 29.9 | |
| **Ga** | 20 | | 22 | | 21 | | 21 | | 22 | | 22 | |
| **Cu** | 36 | | 37 | | 36 | | 10 | | 107 | | 60 | |
| **Zn** | 138 | | 127 | | 127 | | 102 | | 111 | | 115 | |
| **La** | 24.4 | | 27.1 | | 26.1 | | 22.8 | | 27.1 | | 26.0 | |
| **Ce** | 61.6 | | 61.1 | | 52.3 | | 67.2 | | 63.0 | | 63.3 | |
| **ICP Trace Elements (ppm)** | | | | | | | | | | | | |
| **Cs** | 4.39 | 0.323 | 6.46 | 0.170 | 1.024 | 0.657 | 4.50 | 0.351 | 0.313 | 0.105 | 0.363 | 0.097 |
| **Rb** | 26.4 | 30.9 | 26.2 | 20.6 | 20.5 | 28.7 | 30.0 | 33.7 | 33.2 | 36.3 | 30.5 | 38.8 |
| **Ba** | 1780 | 2509 | 1272 | 1087 | 4685 | 1746 | 726 | 745 | 728 | 745 | 655 | 843 |
| **Th** | 2.193 | 1.673 | 2.368 | 2.098 | 2.248 | 2.238 | 1.507 | 1.433 | 2.153 | 1.779 | 1.962 | 1.842 |
| **U** | 0.692 | 0.747 | 0.713 | 0.773 | 0.699 | 0.879 | 0.456 | 0.467 | 0.615 | 0.530 | 0.589 | 0.603 |
| **Nb** | 26.57 | 18.44 | 27.18 | 26.97 | 26.29 | 28.26 | 27.71 | 28.50 | 29.69 | 34.14 | 30.20 | 29.07 |
| **Ta** | 1.853 | 1.251 | 1.901 | 1.917 | 1.809 | 1.987 | 1.959 | 2.255 | 2.092 | 2.461 | 2.097 | 2.275 |
| **La** | 29.14 | 9.63 | 29.18 | 11.86 | 27.73 | 9.90 | 29.15 | 18.28 | 31.92 | 12.49 | 30.45 | 10.06 |
| **Ce** | 62.39 | 17.46 | 62.48 | 22.10 | 59.43 | 18.86 | 62.69 | 35.83 | 67.78 | 25.86 | 65.18 | 20.91 |
| **Pb** | 3.683 | 3.804 | 3.502 | 2.810 | 3.356 | 3.005 | 1.177 | 0.459 | 1.808 | 0.465 | 2.228 | 0.424 |
| **Pr** | 8.01 | 2.15 | 7.98 | 2.65 | 7.61 | 2.31 | 8.02 | 4.27 | 8.55 | 3.27 | 8.32 | 2.70 |
| **Nd** | 36.25 | 9.67 | 36.35 | 11.67 | 34.50 | 10.33 | 35.98 | 18.09 | 37.98 | 14.54 | 37.43 | 12.22 |
| **Sr** | 372 | 356 | 288 | 391 | 440 | 260 | 544 | 278 | 934 | 395 | 775 | 364 |
| **Zr** | 163.1 | 167.2 | 169.5 | 197.6 | 159.7 | 228.1 | 109.9 | 94.6 | 185.9 | 195.9 | 175.7 | 171.4 |
| **Hf** | 4.06 | 4.67 | 4.23 | 5.09 | 3.98 | 5.84 | 2.87 | 2.98 | 4.59 | 4.97 | 4.31 | 4.64 |
| **Sm** | 8.74 | 2.78 | 8.81 | 3.21 | 8.33 | 2.85 | 8.61 | 4.43 | 8.98 | 3.89 | 8.85 | 3.38 |
| **Eu** | 3.424 | 2.277 | 3.484 | 2.264 | 3.331 | 2.061 | 2.939 | 1.828 | 3.198 | 1.281 | 3.028 | 1.147 |
| **Gd** | 7.98 | 2.87 | 8.24 | 3.19 | 7.91 | 2.95 | 8.02 | 4.19 | 8.30 | 3.76 | 8.26 | 3.29 |
| **Tb** | 1.169 | 0.479 | 1.210 | 0.538 | 1.140 | 0.495 | 1.152 | 0.658 | 1.216 | 0.606 | 1.215 | 0.548 |
| **Dy** | 6.54 | 2.96 | 6.69 | 3.28 | 6.34 | 3.05 | 6.30 | 3.78 | 6.78 | 3.51 | 6.65 | 3.33 |
| **Ho** | 1.213 | 0.586 | 1.245 | 0.655 | 1.186 | 0.615 | 1.140 | 0.714 | 1.263 | 0.682 | 1.233 | 0.637 |
| **Y** | 35.30 | 15.53 | 37.48 | 17.89 | 35.55 | 17.04 | 33.17 | 19.77 | 37.41 | 18.94 | 37.08 | 17.94 |
| **Er** | 2.944 | 1.603 | 3.131 | 1.718 | 2.900 | 1.685 | 2.655 | 1.753 | 3.032 | 1.710 | 2.963 | 1.662 |
| **Tm** | 0.398 | 0.238 | 0.407 | 0.254 | 0.379 | 0.246 | 0.346 | 0.237 | 0.390 | 0.238 | 0.386 | 0.237 |
| **Yb** | 2.306 | 1.593 | 2.373 | 1.640 | 2.256 | 1.620 | 1.989 | 1.445 | 2.223 | 1.470 | 2.178 | 1.443 |
| **Lu** | 0.355 | 0.253 | 0.361 | 0.262 | 0.336 | 0.266 | 0.294 | 0.222 | 0.336 | 0.234 | 0.332 | 0.232 |
| **Sc** | 27.4 | 27.8 | 27.6 | 31.2 | 29.1 | 26.1 | 26.9 | 33.5 | 27.8 | 30.5 | 26.9 | 27.2 |
| **87Sr/86Sr** | 0.706337 | 0.706100 | 0.706445 | 0.705898 | 0.706133 | 0.706259 | 0.705900 | 0.705899 | 0.705906 | 0.706184 | 0.705792 | 0.706066 |
| **143Nd/144Nd** | | 0.512598 | | 0.512606 | | 0.512612 | | 0.512740 | | 0.512728 | | 0.512731 |
| **206Pb/204Pb** | | 18.4876 | | 18.4666 | | 18.5096 | | 19.9879 | | 20.3580 | | 20.5031 |
| **207Pb/204Pb** | | 15.5586 | | 15.5536 | | 15.5596 | | 15.6396 | | 15.6576 | | 15.6686 |
| **208Pb/204Pb** | | 38.1543 | | 38.1243 | | 38.1363 | | 39.4972 | | 39.5603 | | 39.6913 |

**Table 3. Sr, Nd and Pb isotope initial and model present day ratios**

| | 88-2L | 88-3L | 88-5L | 99-3L | 99-5L | 99-6L |
|---|---|---|---|---|---|---|
| **Ar40/Ar39 age, my** | 104.7 | 105.9 | 105.3 | 99.7 | 97.8 | 95.9 |
| **Rb, ppm** | 30.87 | 20.61 | 28.66 | 33.66 | 36.34 | 38.82 |
| **Sr, ppm** | 356.0 | 390.6 | 260.4 | 278.1 | 394.7 | 364.4 |
| **Sm, ppm** | 2.782 | 3.212 | 2.855 | 4.432 | 3.888 | 3.379 |
| **Nd, ppm** | 9.67 | 11.67 | 10.33 | 18.09 | 14.54 | 12.22 |
| **Th, ppm** | 1.673 | 2.098 | 2.238 | 1.433 | 1.779 | 1.842 |
| **U, ppm** | 0.747 | 0.773 | 0.879 | 0.467 | 0.530 | 0.603 |
| **Pb, ppm** | 3.804 | 2.810 | 3.005 | 0.459 | 0.465 | 0.424 |
| **238U/204Pb, atoms** | 12.42 | 17.40 | 18.51 | 66.9 | 75.4 | 94.3 |
| **232Th/204Pb, atoms** | 28.75 | 48.8 | 48.7 | 212.2 | 261.4 | 297.8 |
| **232Th/238U, atoms** | 2.314 | 2.804 | 2.631 | 3.173 | 3.468 | 3.157 |
| **87Sr/86Sr measured** | 0.706100 | 0.705898 | 0.706259 | 0.705899 | 0.706184 | 0.706066 |
| **87Sr/86Sr initial** | 0.705726 | 0.705668 | 0.705782 | 0.705402 | 0.705813 | 0.705646 |
| **87Rb/86Sr model** | 0.1328 | 0.1306 | 0.1350 | 0.1203 | 0.1362 | 0.1297 |
| **87Sr/86Sr model present** | 0.705924 | 0.705865 | 0.705984 | 0.705573 | 0.706003 | 0.705822 |
| **143Nd/144Nd measured** | 0.512598 | 0.512606 | 0.512612 | 0.512740 | 0.512728 | 0.512731 |
| **143Nd/144Nd initial** | 0.512479 | 0.512491 | 0.512497 | 0.512643 | 0.512625 | 0.512626 |
| **147Sm/144Nd model** | 0.1941 | 0.1951 | 0.1956 | 0.2080 | 0.2064 | 0.2065 |
| **143Nd/144Nd model present** | 0.512612 | 0.512626 | 0.512632 | 0.512779 | 0.512757 | 0.512756 |
| **206Pb/204Pb measured** | 18.4876 | 18.4666 | 18.5096 | 19.9879 | 20.3580 | 20.5031 |
| **207Pb/204Pb measured** | 15.5586 | 15.5536 | 15.5596 | 15.6396 | 15.6576 | 15.6686 |
| **208Pb/204Pb measured** | 38.1543 | 38.1243 | 38.1363 | 39.4972 | 39.5603 | 39.6913 |
| **206Pb/204Pb initial** | 18.2841 | 18.1784 | 18.2048 | 18.9454 | 19.2056 | 19.0894 |
| **207Pb/204Pb initial** | 15.5488 | 15.5397 | 15.5449 | 15.5896 | 15.6023 | 15.6009 |
| **208Pb/204Pb initial** | 38.0050 | 37.8681 | 37.8820 | 38.4478 | 38.2922 | 38.2752 |
| **238U/204Pb model** | 10.04 | 9.72 | 9.81 | 12.06 | 12.85 | 12.50 |
| **232Th/204Pb model** | 36.20 | 34.70 | 34.90 | 41.00 | 39.32 | 39.12 |
| **206Pb/204Pb model present** | 18.4485 | 18.3394 | 18.3663 | 19.1334 | 19.4021 | 19.2767 |
| **207Pb/204Pb model present** | 15.5567 | 15.5475 | 15.5527 | 15.5986 | 15.6118 | 15.6099 |
| **208Pb/204Pb model present** | 38.1930 | 38.0503 | 38.0643 | 38.6505 | 38.4829 | 38.4612 |
| *** 87Sr/86Sr initial, unleached** | 0.706031 | 0.706049 | 0.705931 | 0.705674 | 0.705763 | 0.705637 |

* (calculated from unleached Rb, Sr and 87Sr/86Sr, Table 2)

Table 1, Supplementary Material: Compositions of Clinopyroxene Phenocrysts and Micro-phenocrysts in one Upper and one Lower Sill sample

| | Normalized Compositions | | | | | | | | | Normalized | Total as | Mg |
|---|---|---|---|---|---|---|---|---|---|---|---|---|
| Sample Number | $SiO_2$ | $TiO_2$ | $Al_2O_3$ | $Cr_2O_3$ | FeO | MnO | MgO | CaO | $Na_2O$ | Total | Measured | Number |
| 88-5, 67-71 | 48.44 | 2.113 | 4.60 | nd | 8.79 | 0.203 | 13.73 | 21.76 | 0.389 | 100 | 100.25 | 0.736 |
| 88-5, 67-71 | 48.54 | 1.975 | 4.58 | nd | 8.82 | 0.167 | 14.16 | 21.38 | 0.371 | 100 | 100.61 | 0.741 |
| 88-5, 67-71 | 47.94 | 2.336 | 4.91 | nd | 9.31 | 0.223 | 13.59 | 21.29 | 0.413 | 100 | 100.84 | 0.722 |
| 88-5, 67-71 | 49.64 | 1.549 | 3.50 | nd | 8.24 | 0.166 | 14.67 | 21.82 | 0.400 | 100 | 100.56 | 0.760 |
| 88-5, 67-71 | 48.66 | 1.946 | 4.47 | nd | 8.77 | 0.178 | 14.07 | 21.62 | 0.300 | 100 | 100.50 | 0.741 |
| 99-6, 24-27 | 48.50 | 2.057 | 4.08 | 0.0045 | 9.62 | 0.187 | 13.80 | 21.37 | 0.377 | 100 | 100.95 | 0.719 |
| 99-6, 24-27 | 48.30 | 2.334 | 4.37 | nd | 9.39 | 0.201 | 13.51 | 21.55 | 0.361 | 100 | 100.09 | 0.719 |
| 99-6, 24-27 | 49.26 | 1.902 | 3.50 | nd | 10.00 | 0.285 | 13.62 | 21.00 | 0.421 | 100 | 101.19 | 0.708 |
| 99-6, 24-27 | 49.83 | 1.607 | 3.29 | nd | 9.02 | 0.221 | 14.39 | 21.27 | 0.364 | 100 | 100.78 | 0.740 |
| 99-6, 24-27 | 48.54 | 2.129 | 4.18 | nd | 9.60 | 0.240 | 13.84 | 21.06 | 0.417 | 100 | 100.42 | 0.720 |
| 99-6, 24-27 | 51.12 | 1.203 | 2.22 | nd | 9.29 | 0.228 | 15.35 | 20.30 | 0.288 | 100 | 100.84 | 0.747 |
| 99-6, 24-27 | 48.48 | 2.156 | 4.34 | nd | 9.72 | 0.218 | 13.93 | 20.70 | 0.453 | 100 | 100.85 | 0.719 |
| Average 88-5 | 48.64 | 1.984 | 4.41 | nd | 8.79 | 0.188 | 14.04 | 21.57 | 0.375 | 100 | 100.55 | 0.740 |
| Average 99-6 | 49.15 | 1.913 | 3.71 | nd | 9.52 | 0.226 | 14.06 | 21.04 | 0.383 | 100 | 100.73 | 0.725 |

Table 2, Supplementary Material

Sample 88-2, 88-92 cm

| Incremental Heating | | | 36Ar(a) | 37Ar(ca) | 38Ar(cl) | 39Ar(k) | 40Ar(r) | Age ±2σ (Ma) | 40Ar(r) (%) | 39Ar(k) (%) | K/Ca ±2σ |
|---|---|---|---|---|---|---|---|---|---|---|---|
| 05C676 | 500 °C | | 0.02648 | 0.29414 | 0.00254 | 0.22782 | 5.45349 | 62.06 ± 2.54 | 41.06 | 5.84 | 0.333 ± 0.028 |
| 05C677 | 600 °C | | 0.00666 | 0.10131 | 0.00108 | 0.13727 | 5.00378 | 93.67 ± 1.52 | 71.75 | 3.52 | 0.583 ± 0.047 |
| 05C678 | 700 °C | | 0.00878 | 0.21558 | 0.00112 | 0.25585 | 9.53207 | 95.68 ± 2.36 | 78.58 | 6.56 | 0.510 ± 0.047 |
| 05C679 | 800 °C | | 0.00768 | 0.37878 | 0.00077 | 0.35532 | 13.85733 | 100.04 ± 1.05 | 85.90 | 9.11 | 0.403 ± 0.034 |
| 05C680 | 875 °C | ✓ | 0.00460 | 0.36499 | 0.00090 | 0.44414 | 18.13876 | 104.63 ± 0.93 | 93.01 | 11.38 | 0.523 ± 0.040 |
| 05C681 | 950 °C | ✓ | 0.00308 | 0.22622 | 0.00163 | 0.64716 | 26.63664 | 105.42 ± 0.66 | 96.67 | 16.59 | 1.230 ± 0.100 |
| 05C682 | 1025 °C | ✓ | 0.00406 | 0.19361 | 0.00220 | 0.66925 | 27.44424 | 105.04 ± 0.67 | 95.79 | 17.15 | 1.486 ± 0.135 |
| 05C683 | 1100 °C | ✓ | 0.00320 | 0.24505 | 0.00119 | 0.54194 | 22.00654 | 104.04 ± 1.11 | 95.86 | 13.89 | 0.951 ± 0.085 |
| 05C684 | 1175 °C | ✓ | 0.00260 | 0.99952 | 0.00119 | 0.55542 | 22.59332 | 104.22 ± 0.62 | 96.69 | 14.24 | 0.239 ± 0.017 |
| 05C685 | 1400 °C | ✓ | 0.00031 | 0.49725 | 0.00016 | 0.06721 | 2.74349 | 104.58 ± 0.73 | 96.72 | 1.72 | 0.058 ± 0.004 |
| | | Σ | 0.06746 | 3.51646 | 0.01278 | 3.90138 | 153.40965 | | | | |

| Information on Analysis | | Results | 40(r)/39(k) ±2σ | Age ±2σ (Ma) | MSWD | 39Ar(k) (%,n) | K/Ca ±2σ |
|---|---|---|---|---|---|---|---|
| Sample | 88-2, 88-92cm | **Weighted Plateau** | 40.8821 ± 0.1690 ± 0.41% | 104.73 ± 1.66 ± 1.59% | 1.93 | 74.98 6 | 0.078 ± 0.088 |
| Material | whole rock | | | External Error ± 2.35 | 2.57 | Statistical T ratio | |
| Location | ODP210-1276 | | | Analytical Error ± 0.42 | 1.3900 | Error Magnification | |
| Analyst | jh | | | | | | |
| Project | ODP 210 | **Total Fusion Age** | 39.3219 ± 0.1432 ± 0.36% | 100.84 ± 1.59 ± 1.58% | | 10 | 0.477 ± 0.014 |
| Irradiation | OSU3F04 | | | External Error ± 2.26 | | | |
| J-value | 0.001462 | | | Analytical Error ± 0.36 | | | |
| Standard | 28.03 | | | | | | |

Sample 88-3, 76-80 cm

| Incremental Heating | | | 36Ar(a) | 37Ar(ca) | 38Ar(cl) | 39Ar(k) | 40Ar(r) | Age ±2σ (Ma) | 40Ar(r) (%) | 39Ar(k) (%) | K/Ca ±2σ |
|---|---|---|---|---|---|---|---|---|---|---|---|
| 05C646 | 500 °C | | 0.04004 | 0.48433 | 0.00426 | 0.28714 | 6.08432 | 54.26 ± 1.68 | 33.95 | 7.56 | 0.255 ± 0.018 |
| 05C647 | 600 °C | | 0.00801 | 0.13358 | 0.00120 | 0.11910 | 3.71017 | 79.22 ± 2.77 | 61.04 | 3.13 | 0.383 ± 0.033 |
| 05C648 | 700 °C | | 0.00234 | 0.04804 | 0.00036 | 0.05276 | 1.88242 | 90.44 ± 1.22 | 73.16 | 1.39 | 0.472 ± 0.035 |
| 05C649 | 800 °C | | 0.00751 | 0.47835 | 0.00143 | 0.43509 | 17.50671 | 101.68 ± 1.50 | 88.73 | 11.45 | 0.391 ± 0.029 |
| 05C650 | 875 °C | ✓ | 0.00319 | 0.18665 | 0.00117 | 0.34873 | 14.55655 | 105.38 ± 1.30 | 93.90 | 9.18 | 0.803 ± 0.062 |
| 05C651 | 950 °C | ✓ | 0.00263 | 0.15669 | 0.00214 | 0.57489 | 24.19418 | 106.22 ± 0.82 | 96.87 | 15.13 | 1.578 ± 0.128 |
| 05C652 | 1025 °C | ✓ | 0.00290 | 0.18016 | 0.00253 | 0.67741 | 28.52114 | 106.26 ± 0.65 | 97.06 | 17.83 | 1.617 ± 0.142 |
| 05C653 | 1100 °C | ✓ | 0.00205 | 0.28191 | 0.00221 | 0.60329 | 25.28643 | 105.80 ± 1.07 | 97.64 | 15.88 | 0.920 ± 0.065 |
| 05C654 | 1175 °C | ✓ | 0.00234 | 1.55100 | 0.00221 | 0.67321 | 28.20720 | 105.76 ± 0.60 | 97.58 | 17.72 | 0.187 ± 0.013 |
| 05C655 | 1250 °C | ✓ | 0.00021 | 0.29844 | 0.00011 | 0.02598 | 1.08689 | 105.60 ± 1.89 | 94.46 | 0.68 | 0.037 ± 0.003 |
| 05C656 | 1400 °C | | 0.00021 | 0.11816 | 0.00000 | 0.00186 | 0.03820 | 52.66 ± 21.41 | 38.08 | 0.05 | 0.007 ± 0.001 |
| | | Σ | 0.07144 | 3.91732 | 0.01764 | 3.79947 | 151.07419 | | | | |

| Information on Analysis | | Results | 40(r)/39(k) ±2σ | Age ±2σ (Ma) | MSWD | 39Ar(k) (%,n) | K/Ca ±2σ |
|---|---|---|---|---|---|---|---|
| Sample | 88-3, 76-80cm | **Weighted Plateau** | 41.9776 ± 0.1408 ± 0.34% | 105.95 ± 1.78 ± 1.68% | 0.55 | 76.42 6 | 0.048 ± 0.064 |
| Material | whole rock | | | External Error ± 2.45 | 2.57 | Statistical T ratio | |
| Location | ODP210-1276 | | | Analytical Error ± 0.35 | 1.0000 | Error Magnification | |
| Analyst | jh | | | | | | |
| Project | ODP 210 | **Total Fusion Age** | 39.7619 ± 0.1495 ± 0.38% | 100.52 ± 1.70 ± 1.69% | | 11 | 0.417 ± 0.014 |
| Irradiation | OSU3F04 | | | External Error ± 2.33 | | | |
| J-value | 0.001441 | | | Analytical Error ± 0.37 | | | |
| Standard | 28.03 | | | | | | |

Sample 99-3, 19-22 cm

| Incremental Heating | | | 36Ar(a) | 37Ar(ca) | 38Ar(cl) | 39Ar(k) | 40Ar(r) | Age ±2σ (Ma) | 40Ar(r) (%) | 39Ar(k) (%) | K/Ca ±2σ |
|---|---|---|---|---|---|---|---|---|---|---|---|
| 05C666 | 500 °C | | 0.01984 | 0.50694 | 0.01851 | 0.22850 | 3.64828 | 40.39 ± 1.67 | 38.35 | 10.46 | 0.194 ± 0.015 |
| 05C667 | 600 °C | | 0.00567 | 0.15032 | 0.00599 | 0.12399 | 3.45112 | 69.83 ± 1.61 | 67.29 | 5.68 | 0.355 ± 0.027 |
| 05C668 | 700 °C | ✓ | 0.00332 | 0.18517 | 0.00318 | 0.16058 | 6.39140 | 99.05 ± 2.67 | 86.66 | 7.35 | 0.373 ± 0.029 |
| 05C669 | 800 °C | ✓ | 0.00339 | 0.37800 | 0.00322 | 0.20696 | 8.28399 | 99.60 ± 1.46 | 89.19 | 9.48 | 0.235 ± 0.017 |
| 05C670 | 875 °C | ✓ | 0.00166 | 0.16580 | 0.00266 | 0.19000 | 7.60424 | 99.59 ± 0.95 | 93.90 | 8.70 | 0.493 ± 0.036 |
| 05C671 | 950 °C | ✓ | 0.00446 | 0.26913 | 0.01137 | 0.39496 | 15.95645 | 100.50 ± 1.07 | 92.35 | 18.08 | 0.631 ± 0.053 |
| 05C672 | 1025 °C | ✓ | 0.00322 | 0.30632 | 0.00918 | 0.43144 | 17.23438 | 99.40 ± 0.88 | 94.75 | 19.75 | 0.606 ± 0.049 |
| 05C673 | 1100 °C | | 0.00127 | 0.33265 | 0.00251 | 0.23933 | 9.21841 | 95.94 ± 0.66 | 96.06 | 10.96 | 0.309 ± 0.022 |
| 05C674 | 1175 °C | | 0.00287 | 1.69468 | 0.00432 | 0.17060 | 6.49935 | 94.92 ± 0.67 | 88.43 | 7.81 | 0.043 ± 0.003 |
| 05C675 | 1400 °C | | 0.00101 | 0.97722 | 0.00171 | 0.03777 | 1.41626 | 93.47 ± 1.34 | 82.64 | 1.73 | 0.017 ± 0.001 |
| | | Σ | 0.04672 | 4.96622 | 0.06267 | 2.18413 | 79.70389 | | | | |

| Information on Analysis | |
|---|---|
| Sample | 99-3, 19-22cm |
| Material | whole rock |
| Location | ODP210-1276 |
| Analyst | jh |
| Project | ODP 210 |
| Irradiation | OSU3F04 |
| J-value | 0.001418 |
| Standard | 28.03 |

| Results | 40(r)/39(k) ±2σ | Age ±2σ (Ma) | MSWD | 39Ar(k) (%,n) | K/Ca ±2σ |
|---|---|---|---|---|---|
| **Weighted Plateau** | 40.0739 ± 0.2097 ± 0.52% | 99.71 ± 1.84 ± 1.84% | 0.75 | 63.36 5 | 0.345 ± 0.138 |
| | | External Error ± 2.43 | 2.78 | Statistical T ratio | |
| | | Analytical Error ± 0.51 | 1.0000 | Error Magnification | |
| **Total Fusion Age** | 36.4923 ± 0.1753 ± 0.48% | 91.02 ± 1.67 ± 1.84% | | 10 | 0.189 ± 0.006 |
| | | External Error ± 2.21 | | | |
| | | Analytical Error ± 0.43 | | | |

Sample 99-6, 24-30 cm

| Incremental Heating | | | 36Ar(a) | 37Ar(ca) | 38Ar(cl) | 39Ar(k) | 40Ar(r) | Age ±2σ (Ma) | 40Ar(r) (%) | 39Ar(k) (%) | K/Ca ±2σ |
|---|---|---|---|---|---|---|---|---|---|---|---|
| 05C657 | 500 °C | | 0.00034 | 0.00621 | 0.00003 | 0.00134 | 0.00952 | 17.87 ± 12.56 | 8.69 | 0.05 | 0.093 ± 0.012 |
| 05C658 | 700 °C | | 0.03756 | 0.52465 | 0.03713 | 0.36419 | 9.92796 | 67.52 ± 1.55 | 47.21 | 13.04 | 0.298 ± 0.024 |
| 05C659 | 800 °C | | 0.00758 | 0.25672 | 0.00893 | 0.16394 | 6.13521 | 92.06 ± 1.08 | 73.23 | 5.87 | 0.275 ± 0.020 |
| 05C660 | 875 °C | ✓ | 0.00322 | 0.16173 | 0.00361 | 0.14055 | 5.58207 | 97.55 ± 2.34 | 85.41 | 5.03 | 0.374 ± 0.028 |
| 05C661 | 950 °C | ✓ | 0.00714 | 0.20625 | 0.01016 | 0.32380 | 12.73494 | 96.63 ± 1.60 | 85.77 | 11.59 | 0.675 ± 0.054 |
| 05C662 | 1025 °C | ✓ | 0.00950 | 0.20076 | 0.00448 | 0.76963 | 30.08815 | 96.07 ± 0.64 | 91.45 | 27.55 | 1.648 ± 0.144 |
| 05C663 | 1100 °C | ✓ | 0.01240 | 0.44426 | 0.00520 | 0.60422 | 23.28570 | 94.74 ± 1.00 | 86.38 | 21.63 | 0.585 ± 0.043 |
| 05C664 | 1175 °C | | 0.02104 | 2.34242 | 0.00643 | 0.37499 | 13.46344 | 88.42 ± 1.75 | 68.40 | 13.42 | 0.069 ± 0.005 |
| 05C665 | 1400 °C | | 0.00569 | 0.98991 | 0.00199 | 0.05071 | 1.82227 | 88.49 ± 1.99 | 51.98 | 1.82 | 0.022 ± 0.002 |
| | | Σ | 0.10448 | 5.13290 | 0.07795 | 2.79338 | 103.04927 | | | | |

| Information on Analysis | |
|---|---|
| Sample | 99-6, 24-30cm |
| Material | whole rock |
| Location | ODP210-1276 |
| Analyst | jh |
| Project | ODP 210 |
| Irradiation | OSU3F04 |
| J-value | 0.001399 |
| Standard | 28.03 |

| Results | 40(r)/39(k) ±2σ | Age ±2σ (Ma) | MSWD | 39Ar(k) (%,n) | K/Ca ±2σ |
|---|---|---|---|---|---|
| **Weighted Plateau** | 39.0069 ± 0.3500 ± 0.90% | 95.86 ± 2.00 ± 2.08% | 2.83 | 65.81 4 | 0.499 ± 0.242 |
| | | External Error ± 2.51 | 3.18 | Statistical T ratio | |
| | | Analytical Error ± 0.84 | 1.6828 | Error Magnification | |
| **Total Fusion Age** | 36.8906 ± 0.1958 ± 0.53% | 90.79 ± 1.78 ± 1.96% | | 9 | 0.234 ± 0.009 |
| | | External Error ± 2.29 | | | |
| | | Analytical Error ± 0.47 | | | |